ORIGINAL PAPER

CrossMark

Secondary dispersion of trace elements in bottom sediments of the High Dam Lake, South Egypt and North Sudan

Mohamed Abdallah Gad Darwish[1] · Hebert Pöllmann[2]

Abstract

Thirty-four chemical elements, pH, total nitrogen, and total organic carbon were determined in 49 bottom sediment samples from the whole High Dam Lake in order to improve our understanding of geochemical characteristics of these sediments and geochemical patterns of trace elements and related feeding sources. The present study revealed that the lake were clearly discriminated into three portions in accordance with the sediment geochemistry and geographic position. Likewise, the analyzed elements in the entire lake sediments were classified into six geochemical association patterns that are indicative of the contributing geogenic and anthropogenic sources. As has been noted here, mineralogy, anthropogenic inputs, pH, and organic matter had significant roles in controlling the behavior, concentration, dispersion, and geochemical patterns of the trace elements in the lake sediments. Consequently, the elevated concentration of Bi, Cd, Co, Cr, Cu, Fe, Ga, Mn, Mo, Ni, Sc, V, Y, and Zn posed moderate contamination level in the sediments. At the same time, the enhancement of Ag, Se, and Te levels caused contamination up to very high levels. Admittedly, the contamination levels were generated by natural and human activities that are coming from the Nile basin countries. Despite progressive deterioration of these sediments, they still have economic applications.

Keywords Secondary dispersion · Statistical techniques · Trace elements · High Dam Lake · South Egypt and North Sudan

Introduction

The lake sediments are considered as the secondary environment for trace elements dispersion, composed of transport materials derived from the watershed (Ng and King 2004), and they undoubtedly are a representative of upstream lithology (Ranasinghe et al. 2009). The composition of lake sediments allows us to understand the fate of transportation of the terrestrial materials into the basins and the factors that control both the distribution and geochemistry of sediments (Hedges and Keil 1995; Bianchi et al. 2002). In addition, the lake sediment

✉ Mohamed Abdallah Gad Darwish
mohamed.darwish26@yahoo.com

[1] Geology Department, Faculty of Science, Aswan University, Aswan 81528, Egypt

[2] Mineralogy and geochemistry department, Faculty of Science III, Halle University, Wittenberg, Halle, Germany

data have been used to study the historical record of heavy metal input to the lakes, evaluate background concentrations, and assess relative increases in concentrations because of large-scale anthropogenic influences (Jin et al. 2006). Consequently, these sediments play a significant role in exploration and environmental geochemistry (Ranasinghe et al. 2009). In the present study, large volumes of the sediments sunk and accumulated in the intact High Dam Lake, which exists beyond the High Dam body, as a result of the sudden decreasing in speed of feeding water of the Sudanese Main Nile due to collision with a huge water mass of this lake. In the entire lake, the amount of sediments was estimated at 125 million tons yearly (Entz 1974), reached 518.2 million m³ in a period between 1987 and 1992 (El Dardir 1994), increased to 6000.2 million m³ in 2007, and enhanced to reach 7 milliard m³ in 2012 as estimated by the Egyptian High Dam Authority. Since more than 70% of the Nile flow sediments were deposited in the upstream part near Wadi Halfa in Sudan (El-Shabrawy 2009), a new Nile delta (ca. 200-km long, mostly subaqueous) was generated between Dal Cataract and Abu Simbel (Mancy and Hafez 1983; El Dardir 1994). Sedimentation processes and related problems and patterns, the progress of the delta formation, and the effects of drought period 1979/1987 in the whole High Dam Lake have

been assessed by Entz (1980); El Dardir (1987, 1994); Makary et al. (2004); the Nile Basin Initiative Transboundary Environmental Action Project (2005); and Moussa (2013).

In the southern part of the High Dam Lake (north Sudan), the mineralogy and the volume of the lake sediments, derived from the Blue Nile, White Nile, and Atbara River, and trapped by Sudanese lake, were estimated by Garzanti et al. (2006, 2015) and Padoan et al. (2011). The most sediments consisted of silts and sands derived from basic and intermediate volcanic rocks and are representative of the provenances of Ethiopia and Sudan with minor contributions from the underlying and surrounding rocks (Ibrahiem et al. 1995). On the other hand, in the middle and northern parts of the High Dam Lake (south Egypt), the mineralogy of their sediments was studied by Philip et al. (1977); El Dardir et al. (1988); Gindy (1991, 2001, 2015); and Ahmed et al. (1993). In fact, the mentioned sediments were a mixture of the Nile sediments and sandstone assemblage and became mostly clayey sediments (Philip et al. 1977; El Dardir 1984). The lake sediments of the study area composed of silt, clay, and sand arranged in their decreasing order of abundance (El Dardir et al. 1988). Other studies revealed that montmorillonite, kaolinite, and illite (Hassan et al. 1977; Sadiek 1987; Khalifa et al. 1994) and smectite (Gindy 2001) are the dominant clay minerals in these sediments.

Many investigations of trace elements in the sediments of the High Dam Lake (south Egypt) have been carried out by Sherief et al. (1978); El Dardir (1984); El Dardir et al. (1988); Zaghloul et al. (1987); Awadallah et al. (1994); Ismail et al. (1994); Ibrahiem et al. (1995); Moalla et al. (1997); Khater et al. (2005); Abou El Ella and El Samman (2010); Darwish (2013); and Goher et al. (2014).

To the authors' knowledge and assessment of the published and none-published literatures of the High Dam Lake, no one has previously carried out geochemical survey for trace elements in the bottom sediments of the entire High Dam Lake. Consequently, the main goal of this manuscript is to (i) determine the baseline levels of the trace elements, (ii) explore the spatial distribution pattern of trace element association and their contribution sources, (iii) determine the mechanism of elemental associations, and (iv) assess the factors controlling their accumulation and dispersion for economic significance and environmental evaluation.

Description of the site

The High Dam Lake exists in the south Aswan city, extending from the High Dam building in the southern part of Egypt until Dahl's cataract in the northern part of Sudan (Fig. 1). The lake trends NE–SW direction and stretches for 480-km long; 300 km in the south Egypt "known as Lake Nasser" and 180 km long in the north Sudan "called Lake Nubia" as seen in Fig. 1b. Only one inflow channel is the Sudanese Main

River drains into this lake and the conspicuous outflow is the High Dam body, which allows pouring the lake water into the Egyptian River Nile.

The High Dam Lake is characterized by a surface area of about 6216 km^2, mean width equals 12.5 km, dendritic shorelines of 9250-km lengths, and a volume of 157 km^3 (Said 1990). It also contains more than 120 billion m^3 of fresh renewable water (Shaltout 1998) and possesses a storage capacity of 164 billion m^3 when water reach a maximum depth of 182 m (Strzepek et al. 2008). Under those circumstances, the study lake is regarded as one of the greatest man-made renewable freshwater reservoirs and the second largest artificial lake in the world (Shaltout 1998) because it was created during the construction of the High Dam building in 1960 and filled with fresh water over the period 1964–1970 (Elsawwaf et al. 2012). Thus, it is essentially considered as the fresh water bank in Egypt.

Due to the situation of the lake in Sahara Desert, the lake is located in a subtropical zone climate based on Köppen-Geiger climatic classification system (McKnight and Hess 2000). The surrounding area of the study lake is generally characterized by an arid climate (hot desert climate), no annual rainfalls, a very scanty shrub, and no land use.

The geology of the area around the High Dam Lake consists of the Precambrian basement rocks of the Arabian-Nubian Shield, which are overlain by Paleozoic, Mesozoic, and Cenozoic sedimentary successions, respectively (Fig. 1b). The Precambrian basement rocks consist mainly of high-grade metamorphic rocks intruded by granite intrusions (El Gaby 1985; El Ramly and Hussein 1985; Khudeir 1983; El Gaby et al. 1990; Garzanti et al. 2006). The sedimentary successions have been investigated by Issawi (1982), Klitzsch et al. (1987), Said (1990), Ibrahiem et al. (1995), Gindy (2001), Garzanti et al. (2006), Sefelnasr (2007), Zaki (2009) ,and Boshnaq (2012). They mentioned that the Paleozoic rocks include Devonian and Carboniferous sandstones; Mesozoic sedimentary successions consist mostly of Upper Jurassic and Lower Cretaceous sandstones; Cenozoic successions are represented by Tertiary rocks "Paleocene shales, limestones, chalky and argillaceous limestones of Paleogene age" and Quaternary deposits "fluvial deposits, piedmont gravels, gravel terraces, Tufas, fresh-water limestones, calcite, Playa deposits, Wadi filling materials, sand sheets and sand dunes of Pleistocene and Holocene ages"; and finally these successions were intruded by Tertiary basaltic rocks.

Methods

Sediment sampling

To achieve the aims of this paper, 49 samples had been collected from the surface layer of the bottom sediment bed
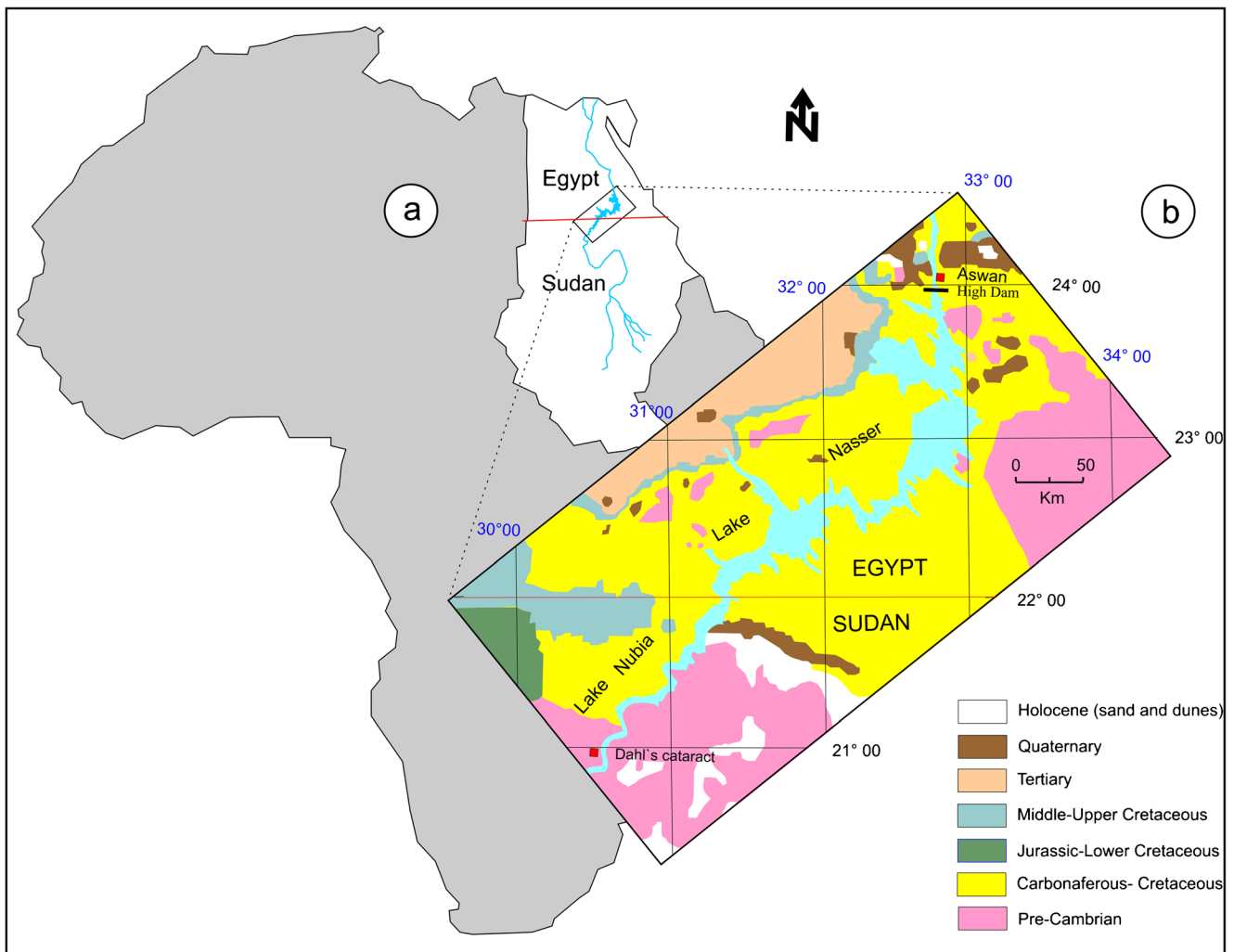
Fig. 1 a Sketch map showing the location of the High Dam Lake in south Egypt and north Sudan. **b** Schematic geological map of the High Dam Lake digitized from maps of CONOCO (1987) and USGS (2004). Outlines of lithologies are explained in the text

covering the whole High Dam Lake: 27 samples from the north and middle parts (Lake Nasser) and 22 samples from the south part (Lake Nubia) (Fig. 2). Sampling of the sediment materials was performed using a grab sampler and the sediments were taken with a plastic spoon to avoid metal contamination. Afterwards, they were placed in PVC bags, stored and frozen at minus 2 °C prior treatments and chemical analyses.

Sediment preparation and analyses

In the laboratory, all samples were defrosted, wet screened to minus 180 μm grain size fraction that is suitable for the geochemical survey, and air-dried at 20 ± 3 °C. A hundred grams of each homogenized and dried subsample obtained by cone and the quarter method was re-dried again in the oven (< 40 °C) to constant weight. Subsequently, 20 g had been ground using the agate mill in order to produce minus 63 μm grain size fraction for chemical digestion. In order to achieve the geochemical

analysis, about 1 g of each produced subsample (minus 63 μm) was used for the inductively coupled plasma mass spectrometry (ICP-MS) determinations at the laboratories of geochemistry of Martin Luther University, Halle-Wittenberg, Germany. Consequently, 34 chemical elements (Au, Ag, Ba, Bi, Cd, Co, Cr, Cu, Fe, Ga, Hf, Hg, Li, Mn, Mo, Nb, Ni, Pb, Rb, Sb, Sc, Se, Sn, Sr, Ta, Te, Th, Ti, Tl, U, V, Y, Zn, and Zr) were analyzed following an HCl–HNO$_3$–H$_2$O (7.2 mL:2.4 mL:1 mL) leaching in the microwave apparatus using a multiple stage program: 6 min at 1000 W (160 °C), 9 min at 1000 W (195 °C), 20 min. at 700 W (195 °C), and 20 min for ventilation. The obtained digested solutions were cooled to room temperature, filtered, rinsed with deionized water for dilution to 50 mL, and then used for chemical analysis.

For Fe determination, a further 1 g of the sub-sample (minus 63 μm) was weighed into 100 mL Pyrex beakers to which 4 mL of (1:1) HNO$_3$ + 10 mL (1:4) HCl were added. The contents were covered by watch glass and heated on a hot

Fig. 2 High Dam Lake map showing the sampling stations for the bottom sediments (closed circle)
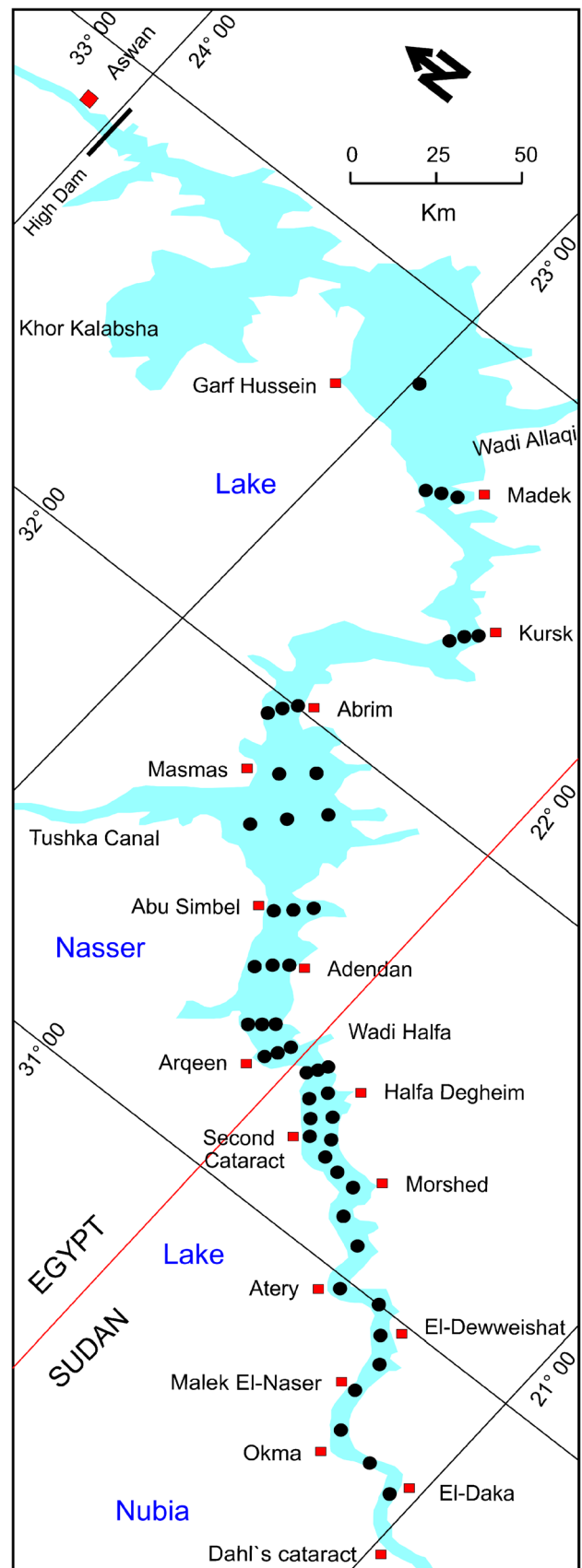
plate at 95 °C for 30 min. The produced digest was cooled, washed with deionized water, filtered, and diluted to 100 mL with the same water (Martin et al. 1994). The obtained clear solutions were analyzed with flame atomic absorption spectrometry (AAS) at Aswan University, Egypt.

In order to measure pH value, 4 g of the sub-sample (minus 63 μm) had been mixed with 80 mL Milli-Q-water, shaken mechanically for 1 h and left for 20 h to settle down. The produced clear solutions were measured for pH values using SCHOTT pH-meter digital instrument at geochemistry laboratories of Martin Luther University, Germany. The recalibration was carried out every 10th sample using standard pH solutions (4 and 7) and measuring pH values for each sample was recorded twice to an accuracy of 0.005 with the mean value being reported.

Finally, for estimation of total organic carbon (TOC) and total nitrogen (TN), inorganic carbonates were expelled by heating the sub-samples (minus 63 μm) with HCl (10 vol.%) on the hot plate at 70 °C to dryness (Gaebler 1997). After cooling, TOC and TN contents were measured using a Vario EL Hanau apparatus at the chemistry department of Martin Luther University, Germany.

The quality control of the chemical analysis had been achieved using international certified reference materials (Buffalo river sediment). In the meantime, duplicate samples, the replicate analyses, and instrumental calibration had been performed in each analytical set. The obtained data were within the 95% confidence limits of the recommended values for the mentioned standard substances. The determination of the chemical elements in THE Buffalo river sediment reference material and Merck multi-elements standard solutions by using ICP-MS instrument gave good results (Table 1).

Statistics

The processing of the obtained geochemical data of 49 lake sediments samples was performed applying statistical treatments, graphic representative plots, and mapping construction. Prior data processing, all analyzed elements notified as being below the detection limit, including Au = 96%, Hg = 77.6%, Sb = 79.6%, and Nb = 41% were removed from the data because they could only give extremely restricted interpretable information. Statistical techniques used here include uni-, bi-, and multi-variate methods for making the geochemical data sets possible to display the distribution of the single element and elemental association, and identify their interrelations and groupings in order to simplify, compare, and summarize these data for the purpose of subsequent interpretation.

Descriptive statistics were calculated, and the normality of the analyzed data was examined using a skewness, kurtosis, and coefficient of variation. The populations of all variables with highly skewed distributions cannot primarily be assumed to be normally distributed. Then, the valid data were logarithmically transformed (base 10) prior applying bi- and multivariate methods. Non parametric statistical hypothesis test, namely Wilcoxon signed-rank test, was used to assess whether their population median ranks differ. To compare the means of analyzed variables and assess the relationship of their concentrations in the sediments of the lake parts for recognizing whether there is a significant difference, one-way ANOVA for raw and log_{10} transformed data (at 95% confidence interval) and Tukey's (HDS) multiple range test were computed. For validating the ability of the instrument to predict concentrating the elements in un-sampled stations near the High Dam, linear regression analysis was used for this purpose.

Bivariate method named Pearson product-moment correlation coefficient was applied to assess the relation between variables' concentrations and the lake parts. Nevertheless, the multivariate statistical methods have been used for reducing the data sets into new homogenous groups according to their geochemical properties and signatures. These methods are represented by: (i) discriminant analysis, which was performed to evaluate the efficacy of stream sediment geochemistry in distinguishing source areas (Rao 1963) and ensure the homogeneity of variance where variables were combined to form discriminant functions that maximized separating the clusters. Here, the sediments of the three parts of the lake were used as the grouping variable and served to validate and supplement the cluster (Norusis 1988). (ii) Factor analysis was used to ensure the homogeneity of variance and further normalize the data (Reimann et al. 2002) as well as to characterize different groups of chemical elements with approximately similar geochemical patterns and gather the associated variables into a few factors (Harman 1970). Each factor can be regarded as a single "type" of sediment produced by a unique mode of formation (Ng and King 2004). Finally, the distribution of elemental association factor scores (produced by R-mode factor analysis) is presented in the form of geochemical maps.

Potential pollution assessment methods

For comprehensive and scientific assessment of potential pollution generated by heavy elements of the lake sediments, single pollution indices (geo-accumulation index (I_{geo}) and contamination factor (C_f^i)) and integrated pollution indices (contamination degree (C_d) and pollution load index (PLI)) have been applied in the present study.

Geo-accumulation index

The geo-accumulation index was used to evaluate the quantification of pollution and related levels caused by the heavy

Table 1 Results of element concentrations in reference material of Buffalo river sediments (8704) and Merck multi-elements standard solutions determined by ICP-MS instrument

Buffalo river sediment				Merck multi-element standards			
Element	Certified value (mg/kg)	Measured mean (mg/kg)	Recovery %	Element	Certified value (mg/l)	Measured mean (mg/l)	Recovery %
Ba	413	398	96.37	Au	1.00	1.045	104.5
Cd	2.94	2.63	89.46	Ag	1.00	1.041	104.1
Co	13.57	10.41	76.71	Bi	10.00	8.798	87.98
Cr	121.9	114.69	94.09	Cu	1.00	1.013	101.3
Hf	8.4	7.18	85.48	Fe[a]	1.00	1.029	102.9
Mn	544	429.81	79.01	Ga	1.00	1.009	100.9
Ni	42.9	39.94	93.10	Hg	1.00	1.056	105.6
Pb	150	133.27	88.85	Li	1.00	0.971	97.1
Sb	3.07	2.92	95.11	Mo	5.00	4.808	96.16
Sc	11.26	8.92	79.22	Nb	1.00	1.119	111.9
Th	9.07	7.24	79.82	Rb	5.00	5.400	108
Ti	0.457	0.37	80.96	Se	1.00	1.075	107.5
U	3.09	2.42	78.32	Sn	5.00	4.650	93
V	94.6	93.88	99.24	Sr	1.00	0.984	98.4
Zn	408	382.62	93.78	Ta	1.00	1.104	110.4
				Te	5.00	4.945	98.9
				Tl	1.00	0.940	94
				Y	1.00	1.061	106.1
				Zr	1.00	1.066	106.6

[a] Determined by AAS, recovery % = (average measured value/certified value) × 100

elements. The mathematical method proposed by Müller (1979) has been applied using the following equation:

$$I_{geo} = Log_2\left[\frac{C_n}{(1.5\,B_n)}\right] \tag{1}$$

where C_n refers to the measured concentration of study element in the sediment, B_n is the geochemical background of an examined element ($_n$), and the factor 1.5 is used for the background matrix correction due to lithogenic influences. Seven categories of I_{geo} suggested by Müller (1981) are identified in Table 2.

Contamination factor

According to Hakanson (1980) and Liu et al. (2005), contamination factor has been computed to describe and assess the contamination of examining toxic elements in the sediments applying the equation as follows:

$$C_f^i = \frac{\overline{C}_{0-1}^i}{C_n^i} \tag{2}$$

where $\overline{C}_{0-1}^i$ is the mean concentration of each element in the sediment and C_n^i refers to a baseline or background value.

Four classes characterized by Hakanson (1980) and Pekey et al. (2004) on the basis of contamination factor levels are given in Table 2.

Contamination degree

Contamination degree can recognize and evaluate the toxic element contamination in the sediments. Based on the method of Hakanson (1980), the contamination degree of the environment can be calculated as the sum of the contamination factors for all elements of interest using this formula:

$$C_d = \sum_{i=1}^{m} C_f^i \tag{3}$$

where C_f^i refers to the contamination factor, and m is the number of the heavy metal species. As seen in Table 2, four contamination degrees have been classified based on the suggestion of Caeiro et al. (2005) and Pekey et al. (2004).

Pollution load index

Cabrera et al. (1999) and Liu et al. (2005) suggested the method of pollution load index calculation in order to provide a simple and comparative evaluation of heavy metal pollution level at each sampling station. The pollution load index can be

Table 2 Terminologies for some single and integrated pollution indices

	Single pollution indices				Integrated pollution indices			
	I_{geo} (Müller 1981)			C_f^i (Caeiro et al. 2005; Pekey et al. 2004)		C_d (Caeiro et al. 2005; Pekey et al. 2004)		PLI (Cabrera et al. 1999; Liu et al. 2005)
	I_{geo} value	Class	Pollution intensity	C_f^i value	Contamination level	C_d value	Contamination level	PLI value	Pollution level
	<0–0	0	Unpolluted	$C_f^i <1$	Low contamination factor	$C_d < m$	Low degree of contamination	0	Perfection[b]
	0–1	1	Unpolluted to moderated	$1 \le C_f^i < 3$	Moderated contamination factor	$m \le C_d < 2\,m$	Moderate degree of contamination	<1	No metal pollution[c]
	1–2	2	Moderated polluted	$3 \le C_f^i < 6$	Considerable contamination factor	$2\,m \le C_d < 4\,m$	Considerable degree of contamination	1	Baseline level[b]/close to background level[d]
	2–3	3	Moderated to heavily polluted	$C_f^i \ge 6$	Very high contamination factor	$C_d \ge 4\,m$	Very high degree of contamination	>1	Pollution exist/progressive deterioration[b]
	3–4	4	Heavily polluted						
	4–5	5	Heavily to extremely polluted[a]						
	>5	6	Extremely polluted[a]						

[a] Suggested by Bhuiyan et al. (2010)
[b] Suggested by Suresh et al. (2011)
[c] Suggested by Chakravarty and Patgiri (2009)
[d] Suggested by Cabrera et al. (1999)

computed as the mth root of the product of the (m) contamination factor (C_f^i) following equation proposed by both authors:

$$\text{PLI} = \left(\prod_{i=1}^{m} C_f^i \right)^{1/m} \qquad (4)$$

where C_f^i refers to the contamination factor of heavy metal i, and m is the count of the heavy metal species. The terminologies of the pollution load index are listed in Table 2.

In this study, the average values of the chemical elements in the upper continental crust of the earth (after Taylor and McLennan 1985, 1995; Hu and Gao 2008) were used as the reference values for their corresponding heavy elements in the High Dam Lake sediments in order to accurately obtain the pollution levels in these sediments. The geochemical data processing was performed by more than one software; XLstat 3.02 and SPSS 16 software for statistical treatment; Coreldraw 12 and Golden Surfer 8 software for graphical and mapping construction.

Results and discussion

Descriptive statistics

The descriptive statistics for the 33 variables determined in the High Dam Lake sediment samples are presented in Supplementary Table 1. This table shows that the geometric mean values of some elements, such as Se (1.120 ppm), Ag (338.81 ppb), Te (0.138 ppm), Ni (53.992 ppm), Co (17.728 ppm), Ga (28.708 ppm), Cr (62.449 ppm), Cu (44.089 ppm), Fe (5.682%), V (88.055 ppm), Cd (0.115 ppm), and Sc (11.695 ppm) are higher than their corresponding average concentrations in the upper continental crust of the Earth (0.05 ppm, 50 ppb, 0.027 ppm, 20 ppm, 10 ppm, 17 ppm, 35 ppm, 25 ppm, 3.5%, 60 ppm, 0.098 ppm, and 11 ppm, respectively). The elevated concentrations are commonly related to either geogenic origin or anthropogenic activities. Since the data was not normal as seen in Supplementary Table 1 and Fig. 3, the data were log transformed.

Wilcoxon signed-rank test

The Wilcoxon signed-rank test computation presents that median of Ag ($p > 0.05$) possesses no significant difference with the median of distance in both raw and $\log_{10}$-transformed data (Supplementary Table 2). This reflects an enhancement of Ag content toward the south part of the lake, revealing that the source of Ag is related to either geologic or anthropogenic particulates in Lake Nubia (Darwish 2013). In a likely manner,

Table 3   Results of linear regression analysis of the High Dam Lake bottom sediments' data and their predicted concentrations (49 samples)

Variable	F value	R^2	Adjusted R^2	p value	Regression, $y = a + bx$	Predicted variables near high dam at distance of 25 km	Unit
Ag	0.000	0.000	-0.021	0.996	$y = 376.147 - 0.002 \times x$	376.11	µg/kg
Ba	0.178	0.004	-0.017	0.675	$y = 155.083 + 0.021 \times x$	155.60	mg/kg
Bi	0.002	0.000	-0.021	0.965	$y = 90.729 + 0.003 \times x$	90.81	µg/kg
Cd	1.936	0.040	0.019	0.171	$y = 138.676 - 0.066 \times x$	137.04	µg/kg
Co	54.686	0.538	0.528	<0.0001	$y = -3384.838 + 76.720 \times x$	-1466.85	µg/kg
Cr	28.232	0.375	0.362	<0.0001	$y = 22,468.736 + 139.805 \times x$	25,963.9	µg/kg
Cu	0.418	0.009	-0.012	0.521	$y = 425 + 14.727 \times x$	42,840.7	µg/kg
Fe	30.340	0.392	0.379	<0.0001	$y = 32,337.50 + 84.455 \times x$	34,448.9	mg/kg
Ga	0.768	0.016	-0.005	0.385	$y = 41,504.455 - 25.943 \times x$	40,855.9	µg/kg
Hf	9.262	0.165	0.147	0.004	$y = 1058.581 - 1.364 \times x$	1024.47	µg/kg
Li	16.194	0.256	0.240	0.0002	$y = 20,526.965 - 25.612 \times x$	19,886.7	µg/kg
Mn	40.713	0.464	0.453	<0.0001	$y = -163.844 + 2.675 \times x$	-96.97	mg/kg
Mo	1.191	0.025	0.004	0.281	$y = -1909.791 + 12.058 \times x$	-1608.34	µg/kg
Ni	7.732	0.141	0.123	0.008	$y = 34,682.228 + 74.387 \times x$	36,541.9	µg/kg
Pb	2.471	0.050	0.030	0.123	$y = 9580.130 - 6.166 \times x$	9426.0	µg/kg
Rb	0.579	0.012	-0.009	0.451	$y = 29,663.411 - 10.336 \times x$	29,405.0	µg/kg
Sc	3.960	0.078	0.058	0.052	$y = 7705.212 + 18.251 \times x$	8161.5	µg/kg
Se	27.523	0.369	0.356	<0.0001	$z = 4609.927 - 9.684 \times x$	4367.8	µg/kg
Sn	0.018	0.000	-0.021	0.893	$y = 1982.447 - 0.149 \times x$	1978.7	µg/kg
Sr	23.908	0.337	0.323	<0.0001	$y = 34,183.921 + 146.639 \times x$	37,849.9	µg/kg
Ta	10.585	0.184	0.166	0.002	$y = 988.763 - 1.258 \times x$	957.31	µg/kg
Te	0.810	0.017	-0.004	0.373	$y = 125.227 + 0.093 \times x$	127.56	µg/kg
Th	0.003	0.000	-0.021	0.960	$y = 5376.213 + 0.188 \times x$	5380.9	µg/kg
Ti	45.871	0.494	0.483	<0.0001	$y = -209.883 + 3.650 \times x$	-118.62	mg/kg
Tl	0.584	0.012	-0.009	0.448	$y = 239.976 - 0.091 \times x$	237.70	µg/kg
U	14.808	0.240	0.240	0.0004	$y = 649.308 + 2.837 \times x$	720.23	µg/kg
V	51.453	0.523	0.512	<0.0001	$y = -30,358.051 + 423.045 \times x$	$-19,781.9$	µg/kg
Y	5.436	0.104	0.085	0.024	$y = 16,041.807 + 27.303 \times x$	16,724.4	µg/kg
Zn	20.009	0.299	0.284	<0.0001	$y = 34,834.648 + 122.390 \times x$	37,894.4	µg/kg
Zr	0.065	0.001	-0.020	0.800	$y = 25,160.180 - 3.658 \times x$	25,068.7	µg/kg
pH	115.07	0.71	0.704	<0.0001	$y = 6.607 + 0.004 \times x$	6.71	Unity
TOC	85.823	0.646	0.639	<0.0001	$y = 2.207 - 0.004 \times x$	2.11	wt%
TN	51.325	0.522	0.512	<0.0001	$y = 1.120 - 0.002 \times x$	1.07	wt%

pH a logarithmic measure of hydrogen ion concentration, *TOC* total organic carbon, *TN* total nitrogen, *a* the *y*-intercept, *b* the slope, *x* the independent or predictor variable (distance), *y* the dependent or response variable

the median values of Hf, Mo, and Ta display no significant difference with those of Mn (raw data and $\log_{10}$ data), except for Ta (*p* value > 0.05). As well, the median values of Cr and Ni do not show a statistically significant difference with the median of Fe (raw data) while Cr and Zn give the same result with the logarithm data of Fe. Thus, it is more realistic to accept the null hypothesis and this reflects that the elements: Cr, Hf, Mo, Ni, Ta, and Zn have close relation with detritus Fe and Mn minerals. On the contrary, other concerned elements exhibit significant statistical differences of their medians with those of distance, Fe, Mn, pH, TN, and TOC (*p* values < 0.05), rejecting the null hypothesis.

One-way ANOVA

One-way ANOVA and mean comparisons calculation of the examining variables expect that the variables' contents in the north, middle, and south parts of the lake should be different, despite this contravenes with the null hypothesis adopted here. Indeed, most variables reject the null hypothesis, but the remaining elements, particularly Ag, Ba, Cd, Ga, Mo, Pb, Rb, Tl, and Zr accept it (Supplementary Table 3). Regarding the results of $\log_{10}$ data, they give the same results except Mo because the latter acquires the *F* value of about 12 times exceeding that of the raw data. In Supplementary Table 3,
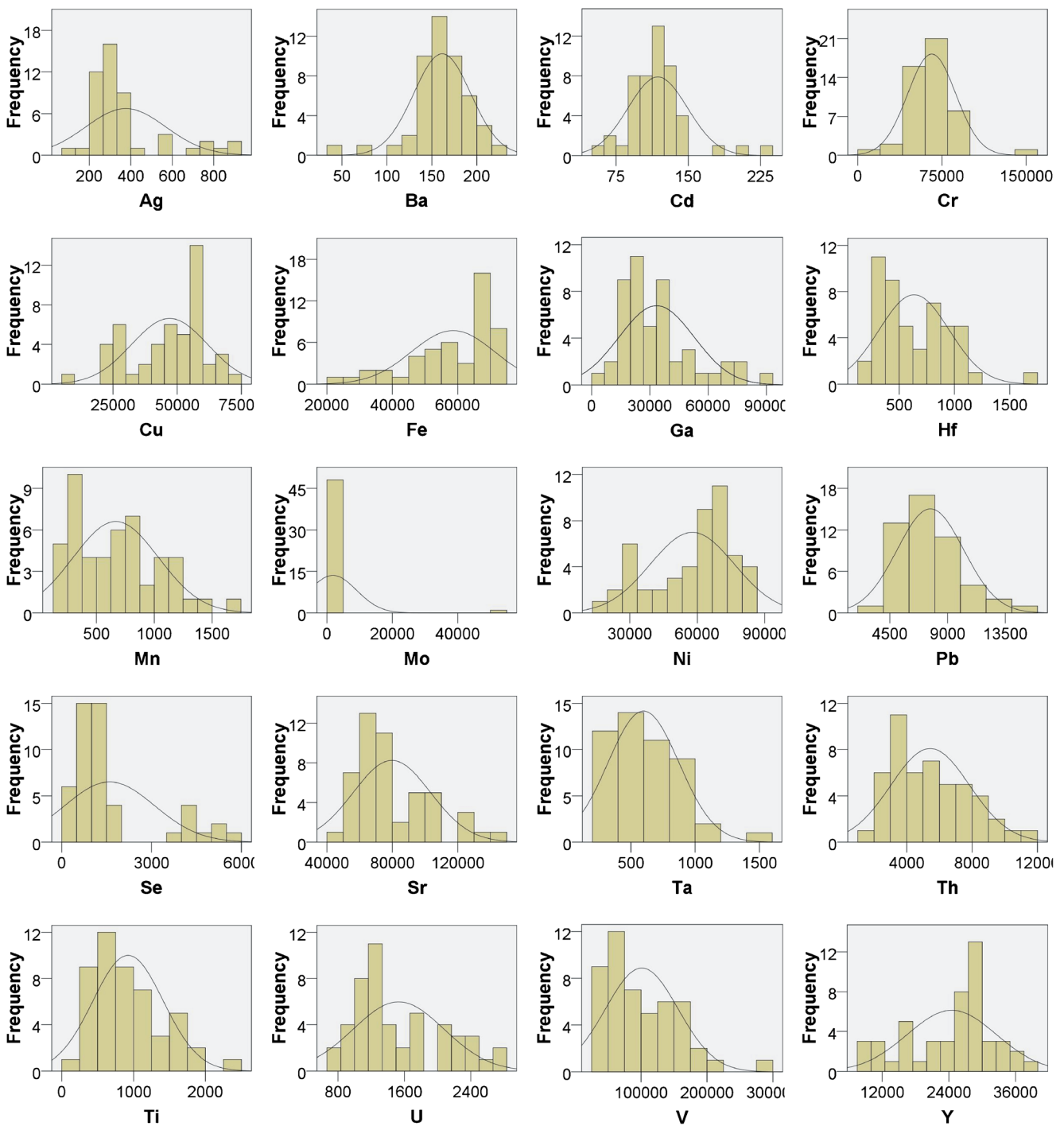
Fig. 3 Histograms with their superimposed normal fitting curves of Ag and some selected elements in the bottom sediments of the High Dam Lake

based on the raw and $\log_{10}$ converted data, more than half of elements possesses the p values below 0.05 and various F values. Also pH, TN, and TOC possess the similar difference, although they have p values equal to zero, high F values, and little variation in their mean ± SE values within the lake parts. In brief, these results support the significant difference of the considered variables and geochemistry of the sediments in the three parts of the High Dam Lake. This

reveals that the geographic and geological effects on levels and dispersions of the mentioned variables are considerably strong.

Linear regression analysis

The correlation relationships between the analyzed variables and the downstream distance of the study lake were

Fig. 4 Scatter plot showing the relation between Fe/Mn ratios and their corresponding distance in the bottom sediments of the High Dam Lake
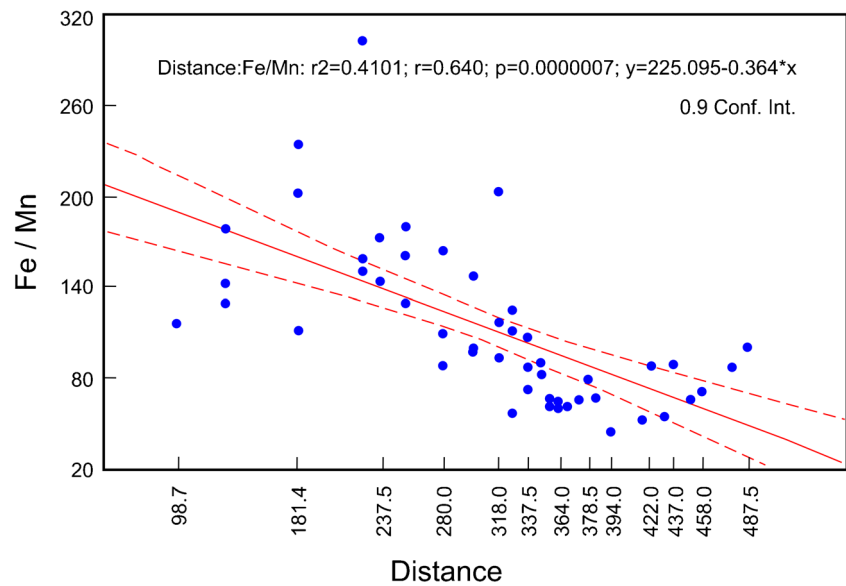
estimated using the linear regression analysis (Table 3). The concentration of about half variables shows upstream decreasing trend; however, the remaining variables (Ag, Co, Cr, Cu, Hf, Mn, Mo, pH, Se, Sr, Ti, TN, TOC, U, V, and Zn) increase southward. Consequently, Fe, Mn, pH, TOC, and Fe/Mn ratio (Figs. 3 and 4) could play an essential role in controlling the concentrations and distributions of the concerned elements, and geochemical nature of the sediments within the lake parts. This finding is powered by (i) the positive correlation of Fe with Mn, Co, Cr, and Zn ($r^2 = 0.679$, 0.513, 0.342, 0.278, respectively); (ii) Mn is positively correlated with Co, Fe, V, Ti, Zn, and Cr ($r^2 = 0.786$, 0.0.679, 0.510, 0.507, 0.478, 0.448, respectively); (iii) the total organic carbon is positively correlated with Mo, TN, Ti, V, Cr, and Se ($r^2 = 0.475$, 0.363, 0.308, 0.303, 0.243, 0.234, respectively); and (iv) pH exhibit positive correlation with V, Ti, TOC, TN, Mn, Co, Zn, Cr, and Sr ($r^2 = 0.614$, 0.598, 0.514, 0.577, 0.415, 0.360, 0.280, 0.272, 0.254, respectively). It is important to mention that the present results are in agreement with the suggestion of Reedman (1979) who revealed that the role of organic matter in the secondary dispersion is extremely considerable to form element-organic complexes and the role of pH at which the hydroxide of the mentioned elements precipitated as known as the pH of hydrolysis. In addition, these results are also in accordance with propositions of Holmström and Öhlander (2001), Land et al. (2002), and Ávila et al. (2005) who detected that co-precipitation or adsorption of those elements were occurred by Fe and Mn oxides, hydroxides, and oxyhydroxides.

The prediction for Bi, Sn, Th, and Zr values in the sediments is clearly the poorest among the group of remaining elements (p value ≥ 0.8 and $R^2 = 0$) as indicated by their concentrations increase northward due to the presence of fine-grained minerals, mud fraction, colloidal particles, and clay minerals. These materials control element concentrations and their dispersions via adsorption on these particulates that hold cations by virtue of unsatisfied electric charges at crystal edges and within the lattice layers (Hirst 1962; Reedman 1979).

Pearson's correlation coefficient

Concerning the relationship between the variables' levels and the lake parts as obtained by the matrix of Pearson's correlation coefficients (Table 4). Firstly, the northern part of the lake is positively correlated with TN, Se, TOC, Mo, Ta, and Hf, indicating the important function of organic matter to accumulate and scavenge the associated elements (Hirst 1962; Davis and Leckie 1978; Kaiser and Zech 2000; Pokrovsky and Schott 2002). Secondly, the middle part of the lake is positively correlated with Th, Bi, Sn, and Li, suggesting a presence of carbonates and detritus Sn-bearing minerals (Ionov et al. 1993; Jiang et al. 2004; Norra et al. 2006), K-feldspare (Garzanti et al. 2006) and monazite. Thirdly, the southern part (Lake Nubia) has positive correlation with V, Mn, pH, Co, Ti, Sr, Zn, Cr, Te, Fe, Ni, U, and Cu, reflecting that the considered elements were trapped by detrital Fe–Mn minerals (Fe and Mn oxides, hydroxides, and oxyhydroxides) with significant roles of pH values (Rovira et al. 2008). As well, these elements were derived from Fe–Ti–Cr oxides (Garzanti et al. 2015), titanite (Padoan et al. 2011), rutile, ferromagnesian minerals and rock fragments, and grains represented by volcaniclastic mud and metamorphiclastic sand (Padoan et al. 2011), and fragments of volcanic and basement rocks (Garzanti et al. 2006) existed in the sediments of Atbra River, the Blue Nile, and the main Nile.

Table 4 Pearson product moment correlation matrix between variables' concentrations and three parts of the High Dam Lake (log₁₀ data, 49 samples)

Variable	North	Middle	South
Ag	0.129	− 0.018	− 0.074
Ba	− 0.115	0.049	0.032
Bi	*− 0.302*	*0.494*	*− 0.275*
Cd	0.087	− 0.021	− 0.040
Co	*− 0.367*	*− 0.456*	*0.709*
Cr	*− 0.542*	− 0.147	*0.526*
Cu	0.130	*− 0.386*	0.290
Fe	*− 0.648*	0.024	*0.432*
Ga	0.206	*− 0.296*	0.147
Hf	*0.379*	0.051	*− 0.317*
Li	0.134	*0.457*	*− 0.545*
Mn	*− 0.546*	*− 0.326*	*0.706*
Mo	*0.453*	− 0.179	− 0.142
Ni	− 0.158	*− 0.288*	*0.395*
Pb	0.144	0.191	*− 0.290*
Rb	− 0.014	0.114	− 0.103
Sc	*− 0.625*	0.214	0.229
Se	*0.608*	*− 0.349*	− 0.082
Sn	*− 0.489*	*0.480*	− 0.130
Sr	0.033	*− 0.663*	*0.632*
Ta	*0.385*	0.113	*− 0.383*
Te	0.118	*− 0.611*	*0.521*
Th	*− 0.524*	*0.661*	− 0.284
Ti	*− 0.425*	*− 0.381*	*0.675*
Tl	− 0.051	0.212	− 0.173
U	− 0.189	− 0.220	*0.351*
V	*− 0.329*	*− 0.519*	*0.744*
Y	*− 0.686*	0.244	0.241
Zn	− 0.128	*− 0.517*	*0.600*
Zr	0.051	− 0.018	− 0.018
pH	*− 0.526*	*− 0.333*	*0.699*
TOC	*0.538*	0.053	*− 0.431*
TN	*0.638*	0.108	*− 0.556*

Italic numbers are significant correlated at $p < 0.05$

pH a logarithmic measure of hydrogen ion concentration, *TOC* total organic carbon, *TN* total nitrogen

Discriminant analysis

The classification matrix of the discriminant function analysis (Table 5) exhibits the classification of the lake sediment geochemistry and related sampling locations into the three divisions with an overall accuracy of 95.9 (of cross-validated grouped cases) and 100% (of original grouped cases) with attention to most significant misclassifications include assigning nearly 5% of the middle part samples as the south part samples and vice versa.

Table 5 Classification table of discriminant function analysis of the High Dam Lake bottom sediments' data (log₁₀, 49 samples)

Lake parts			Predicted group membership			Total
			North	Middle	South	
Original	Count	North	7	0	0	7
		Middle	0	20	0	20
		South	0	0	22	22
	%	North	100	0	0	100
		Middle	0	100	0	100
		South	0	0	100	100
Cross-validated[a]	Count	North	7	0	0	7
		Middle	0	19	1	20
		South	0	1	21	22
	%	North	100	0	0	100
		Middle	0	95	5	100
		South	0	4.5	95.5	100

100.0% of original grouped cases correctly classified. 95.9% of cross-validated grouped cases correctly classified

[a] Cross validation is done only for those cases in the analysis. In cross validation, each case is classified by the functions derived from all cases other than that case

Therefore, the inspection of these specific cases shows that fewer than 10% of the misclassified samples exist on the uncertain and broad boundaries among the lake parts.

Regarding to the structural matrix of the discriminant analysis, Table 6 displays two functions as follows: function (1) is responsible for 77.07% of the variance and is high in Y, Sc, Fe, Th, Sn, Cr, Mn, pH, and Ti, and low in Hf, Mo, TOC, TN, and Se. It separates the elements complexed with organic matter from those associated with the detrital heavy minerals, ferromagnesian minerals, and Fe and Mn materials. Where Y, Sc, and Th are accommodated in monazite structure (Gramacciol and Segalstad 1978; Park and Cha 1999) and Fe, Sn, Y, Sc, and Th could be detected in cassiterite as substituting elements (Masau et al. 2000; Jiang et al. 2004). In the same fashion, Fe and Mn were recorded in the detritus mineral structure (Gaspar and Wyllie 1984; Schroeder et al. 2002) when (i) the diffusion of oxidized Fe and Mn from the ilmenite grain structures had occurred (Gaspar and Wyllie 1984; Schroeder et al. 2002) and (ii) ilmenite altered to leucoxene, rutile, anatase, and hematite (Mücke and Bhadra Chaudhuri 1991; Suresh Babu et al. 1994), and goethite and MnO_2 precipitated (Schroeder et al. 2002). At this instant, the produced secondary Fe and Mn materials able to co-precipitate or adsorb the associated elements with a function of pH (Holmström and Öhlander 2001; Land et al. 2002; Ávila et al. 2005; Rovira et al. 2008). The element association in this function was essentially derived from Fe–Ti–Cr oxides of Sudanese country (Garzanti et al. 2015), titanite, monazite, volcaniclastic

Table 6 Structure matrix of discriminant function analysis of the High Dam Lake bottom sediments' data ($\log_{10}$, 49 samples)

Structure matrix

Variable	Function	
	1	2
Ag	− 0.124	0.049
Ba	0.115	− 0.008
Bi	0.367	*0.370*
Cd	− 0.085	0.023
Co	0.266	*− 0.681*
Cr	*0.482*	− 0.441
Cu	− 0.187	− 0.345
Fe	*0.610*	− 0.314
Ga	− 0.243	− 0.208
Hf	*− 0.346*	0.254
Li	− 0.048	*0.559*
Mn	*0.456*	− 0.635
Mo	*− 0.454*	0.046
Ni	0.099	− 0.391
Pb	− 0.103	0.280
Rb	0.032	0.115
Sc	*0.621*	− 0.099
Se	*− 0.628*	− 0.055
Sn	*0.539*	0.257
Sr	− 0.143	*− 0.692*
Ta	− 0.341	0.323
Te	− 0.214	*− 0.593*
Th	*0.602*	0.432
Ti	0.333	*− 0.630*
Tl	0.083	0.200
U	0.140	− 0.335
V	0.220	*− 0.728*
Y	*0.684*	− 0.098
Zn	0.032	*− 0.620*
Zr	− 0.051	0.008
pH	*0.436*	− 0.632
TOC	*− 0.494*	0.339
TN	*− 0.579*	*0.450*

Pooled within-groups correlations between discriminating variables and standardized canonical discriminant functions. Largest absolute correlation between each variable and any discriminant function are in italics

pH a logarithmic measure of hydrogen ion concentration, *TOC* total organic carbon, *TN* total nitrogen

mud, and metamorphiclastic sand from the main Nile, Atbara River, and the Blue Nile (Padoan et al. 2011). Additionally, it was sourced by volcanic rock fragments, olivine, and pyroxene of basaltic rocks from Atbara River, hornblende of basement rocks from the Blue Nile, and Eolian sand (Garzanti et al. 2006).
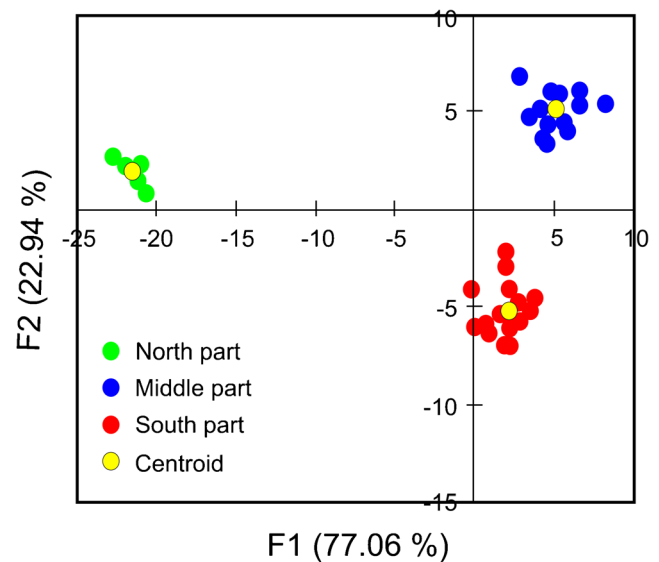

Fig. 5 Plot of canonical discriminant functions 1 vs 2 from discriminant function analysis of the geochemical data matrix of the High Dam Lake bottom sediments

Function (2) describes 22.94% of the total variance and contains high positive correlations among Li, TN, Th, and Bi. In fact, Bi is a main constituent of bismutite while Li accommodate in calcite (Mason 1987) and K-feldspar existed in the Blue Nile sediments (Garzanti et al. 2006). Moreover, clay minerals and clay particles have the ability to adsorb Li, Th and Bi (Hirst 1962; Sahu and Mukherjii 1983; Rath et al. 2009), and TN (Prost et al. 1998; Rožić et al. 2000). For that reason, it is more realistic to mention the importance of clay minerals, mud fraction, and fine particles that trap the elements discriminated in this function either by selective adsorption or combined structurally in their lattices (Hirst 1962; Hall et al. 1998; Reith et al. 2005; Rath et al. 2009). This interpretation is more accepted since the bottom sediments of the lake under investigation are mostly clayey sediments (Philip et al. 1977; El Dardir 1984) and contain carbonate minerals as well.

Figure 5 presents that function 1 discriminates the sediments of both the middle and south parts from the sediments deposited in the north part of the lake and function 2 helps in separating the sediments accumulated in both the north and middle parts from those deposited in the south part of the lake. The remarkable strong and clear separation of three parts of the lake without overlapping refers to the variation in the geochemistry of the lake sediments that were sourced by various lithological inputs besides anthropogenic contributions of the Nile basin countries. Eventually, the performed discriminant analysis succeeded to recognize the Lake Nasser from Lake Nubia and this discrimination is compatible with the geographic position of both Lakes.

Table 7 Rotated component matrix of factor analysis of the High Dam Lake bottom sediments' data ($\log_{10}$, 49 samples)

Variable	Component						Communality
	1	2	3	4	5	6	
Ag	0.034	−0.292	0.041	*0.675*	0.101	−0.419	0.729
Ba	0.355	*0.790*	0.076	−0.229	0.163	−0.077	0.840
Bi	−0.228	0.313	0.384	−0.129	*0.650*	−0.261	0.804
Cd	0.095	0.293	0.048	0.169	−0.064	*0.648*	0.550
Co	*0.937*	−0.161	0.107	0.118	0.124	−0.007	0.945
Cr	*0.695*	−0.042	0.398	−0.225	0.123	0.097	0.719
Cu	*0.800*	0.369	−0.308	0.071	−0.179	0.122	0.922
Fe	*0.729*	0.266	*0.535*	−0.186	0.145	0.006	0.944
Ga	*0.613*	0.426	−0.506	−0.204	−0.225	−0.046	0.906
Hf	−0.110	0.140	0.072	*0.932*	−0.134	0.032	0.924
Li	−0.120	*0.814*	0.215	0.190	−0.397	0.094	0.925
Mn	*0.840*	−0.057	0.327	−0.099	0.214	0.100	0.881
Mo	−0.054	0.351	−0.433	0.205	0.118	0.111	0.382
Ni	*0.889*	0.280	−0.051	−0.014	−0.134	0.046	0.892
Pb	0.141	*0.529*	0.052	0.281	−0.506	0.111	0.650
Rb	0.345	*0.848*	0.033	−0.039	−0.244	0.028	0.901
Sc	0.287	0.124	*0.869*	0.169	0.122	0.183	0.930
Se	0.010	0.396	−0.761	−0.296	−0.047	0.282	0.906
Sn	0.094	*0.531*	*0.772*	−0.066	−0.059	0.081	0.901
Sr	0.449	−0.339	−0.397	−0.154	*0.515*	0.004	0.763
Ta	−0.181	0.193	0.058	*0.903*	−0.078	0.033	0.896
Te	0.287	−0.067	−0.404	−0.319	0.305	*0.501*	0.697
Th	−0.185	0.059	*0.832*	0.184	−0.132	−0.177	0.812
Ti	*0.718*	−0.517	0.106	−0.032	−0.019	0.094	0.805
Tl	0.085	*0.869*	0.244	0.001	0.214	0.181	0.901
U	0.139	−0.200	0.085	0.040	*0.852*	0.105	0.805
V	*0.668*	−0.604	0.076	0.115	0.210	0.033	0.875
Y	0.179	0.020	*0.881*	0.135	0.265	0.111	0.909
Zn	*0.935*	0.013	−0.149	−0.020	−0.033	−0.006	0.898
Zr	0.153	0.027	0.232	*0.768*	−0.009	0.256	0.733
pH	0.440	−0.759	0.179	−0.171	0.214	−0.109	0.889
TOC	−0.206	*0.757*	−0.219	0.285	−0.100	0.269	0.827
TN	−0.387	0.435	−0.408	0.177	−0.289	0.291	0.706

Extraction method: principal component analysis. Rotation method: varimax with Kaiser normalization. Rotation converged in eight iterations; factor loadings exceeding the absolute value of 0.5 are written in italics

pH a logarithmic measure of hydrogen ion concentration, *TN* total nitrogen, *TOC* total organic carbon

Factor analysis

Six rotated factor loadings were successfully extracted from 33 variables (Table 7) with the criterion of an eigenvalue ≥ 1 (Fig. 6) and explained 82.33% of the total variance as reported in Table 8. The results of KMO (Kaiser-Maeyer-Olkin measure of sampling adequacy) and Bartlett's test of sphericity in the present research were 0.567 and 2281.226 ($p < 0.05$), respectively, indicating that the applied factor analysis is useful for the dimensionality reductions. Therefore, the generated factor scores' associations were plotted in the form of geochemical maps (Figs. 7a–c and 8a–c) with conspicuous threshold values identified at 95th percentile. Factor scores association F1 (Co–Zn–Ni–Mn–Cu–Fe–Ti–Cr–V–Ga) accounts for 22.75% of the total variance (Tables 7 and 8) and is characterized by factor scores' values exceeding unity as observed in the sediments of the south part (Lake Nubia) while the lower scores' values move away toward the middle and northern parts of the lake (Lake Nasser) (Fig. 7a). The element association of factor scores F1 is possibly controlled

Fig. 6 Scree plot for the factor analysis (varimax rotation) with all variables (33) of $\log_{10}$ transformed data of the bottom sediments of the High Dam Lake
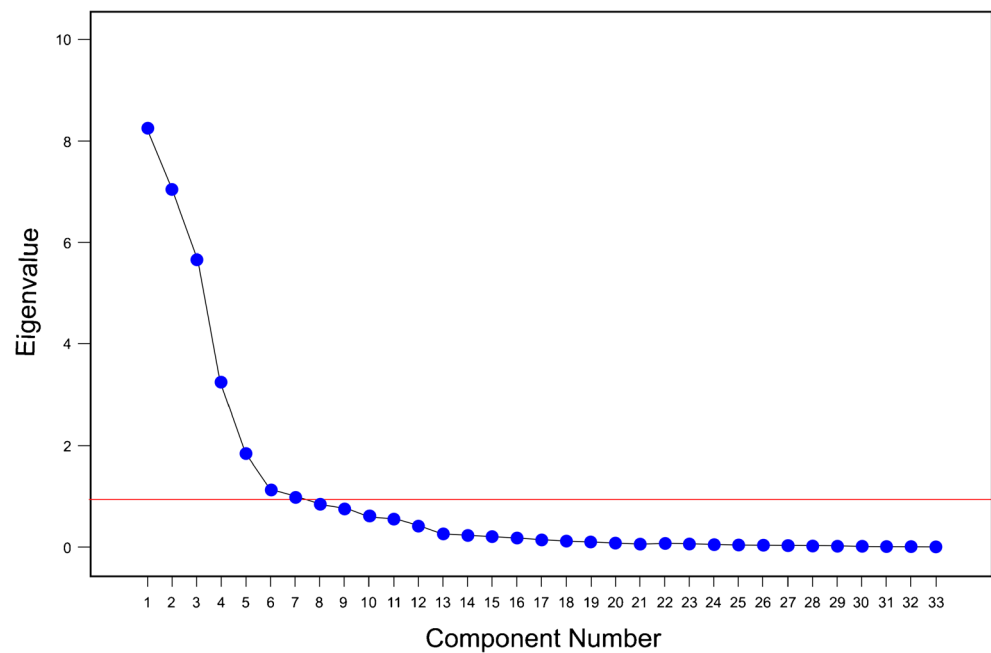
by detrital hematite, magnetite, ilmenite, pyroxene, tourmaline, amphibole, epidote, zoisite, garnet, biotite, rutile, and staurolite (Gindy 2001; Garzanti et al. 2006), Fe–Ti–Cr oxides (Garzanti et al. 2015), titanite, monazite, volcaniclastic mud and metamorphiclactic sand (Padoan et al. 2011), volcanic rock fragments (Garzanti et al. 2006), and Eolian sands (Garzanti et al. 2006; Boshnaq 2012). The mentioned geologic materials were recorded in the lake and considered as the main sources of these elements. With respect to clay minerals, fine-grained minerals and mud fraction, they should be taken into account because they are considered to play a role in scavenging the trace elements in the lake sediments.

Factor scores association F2 (Tl–Rb–Li–Ba–TOC–Sn–Pb) explains 19.93% of the total variance (Tables 7 and 8) and clearly appears in the sediments of the middle part of the lake (Fig. 7b). It refers to a spatial correlation with carbonate materials, calcareous grains, K-feldspar, detrital mica, and organic matter because Ba, Pb, Li, and Rb are related to carbonate materials (Mason 1987; Ionov et al. 1993) and K-feldspar from the Blue Nile (Garzanti et al. 2006), and Sn is controlled by calcareous detritus grains (Hirst 1962). Moreover, all elements associated in this factor can be influenced by organic matter (Hirst 1962; Xiangping et al. 2012) because it has ability to form complexation with these elements by means of adsorption processes (Davis and Leckie 1978; Pokrovsky and Schott 2002). It found that the organic matter can be adsorbed on clay minerals (Kaiser and Zech 2000), finer fractions which have a good correlation with organic matter (Rath et al. 2009), quartz grains (Gindy 2015), calcite, dolomite, and magnesite of lithogenic sources (Thomas et al. 1993) and atmospheric relevant particles that added to the bottom lake (Grassian 2001).

Factor scores association F3 (Y–Sc–Th–Sn–Fe) interprets 16.50% of the total variance (Tables 7 and 8) and the highest F3 factor scores (reach 1.4) scatter along the sediments of the middle part of the lake (Fig. 7c). This association can be explained by the presence of resistant accessory minerals like monazite, titanite, xenotime, and cassiterite that introduced into the lake by geogenic factors. This is supported by (i) the elemental association could be detected in cassiterite (Jiang et al. 2004) in which Fe was dominant substituting element (Masau et al. 2000); (ii) Fe, Y, and Sn are common impurities in titanite from the sediments of Atbara River, the Blue Nile, and the main Nile (Padoan et al. 2011); (iii) Y, Sc, and Th accommodated in monazite structure (Gramacciol and Segalstad 1978; Park and Cha 1999); and (iv) Th and Y existed in xenotime structure (Asami et al. 2002).

Factor scores association F4 (Hf–Ta–Zr–Ag) clears 10.90% of the total variance (Tables 7 and 8). The related high values are monitored in the sediments of the middle and the north parts of the High Dam Lake (Fig. 8a) owing to geologic and anthropogenic activities. For instance: (i) Hf, Ta, and Zr are indicative of detritus zircon grains in which substitution occurred in their structure either by simple or coupled substitution mechanism (de Barros et al. 2010); (ii) Ag can be liberated by rapid oxidation of galena and dispersed into the secondary environment (Yilmaz 2003); and (iii) Ag might be derived from anthropogenic particulate generated by human activities such as medical wastes of hospital laboratories, chiefly radiographic films (Rantitsch 2004), and industrial radiography applications. In the latter two cases of Ag produced by geogenic and anthropogenic factors, Ag can be captured and transported by clay minerals and mud fractions from the south part to reach the middle and north parts of the

Table 8 Total variance explained in factor analysis of the High Dam Lake bottom sediments' data ($\log_{10}$, 49 samples)

Component	Initial eigenvalues			Extraction sums of squared loadings			Rotation sums of squared loadings		
	Total	% of Variance	Cumulative %	Total	% of Variance	Cumulative %	Total	% of Variance	Cumulative %
1	8.259	25.027	25.027	8.259	25.027	25.027	7.506	22.747	22.747
2	7.048	21.357	46.384	7.048	21.357	46.384	6.576	19.927	42.674
3	5.665	17.166	63.550	5.665	17.166	63.550	5.445	16.500	59.174
4	3.251	9.851	73.401	3.251	9.851	73.401	3.598	10.903	70.076
5	1.845	5.590	78.991	1.845	5.590	78.991	2.595	7.864	77.941
6	1.101	3.336	82.327	1.101	3.336	82.327	1.447	4.386	82.327
7	0.994	3.011	85.338						
8	0.846	2.563	87.901						
9	0.749	2.269	90.170						
10	0.616	1.866	92.036						
11	0.552	1.674	93.710						
12	0.411	1.246	94.956						
13	0.253	0.766	95.722						
14	0.228	0.691	96.413						
15	0.214	0.648	97.061						
16	0.189	0.572	97.633						
17	0.142	0.429	98.062						
18	0.116	0.351	98.414						
19	0.095	0.288	98.702						
20	0.081	0.246	98.947						
21	0.066	0.200	99.148						
22	0.058	0.176	99.324						
23	0.055	0.168	99.492						
24	0.043	0.130	99.623						
25	0.033	0.101	99.723						
26	0.025	0.076	99.800						
27	0.020	0.060	99.859						
28	0.014	0.044	99.903						
29	0.012	0.036	99.939						
30	0.009	0.026	99.965						
31	0.006	0.019	99.984						
32	0.004	0.013	99.996						
33	0.001	0.004	100.000						

Extraction method: principal component analysis. Rotation method: varimax with Kaiser normalization

High Dam Lake. Also, Ag could combine with sulfide, bicarbonate, or sulfate, as part of more complex ions or adsorbed onto particulate matter (Eisler 1996).

Factor scores association F5 (U–Bi–Sr) demonstrates 7.86% of the total variance (Tables 7 and 8) and commonly exists in the sediments of the Lake Nubia (Fig. 8b). This association seems to be controlled by detrital carbonate minerals and is a sign to support the lithologic source here in view of the substitution of tetravalent uranium for divalent calcium occurred in calcite structure, and subsequently tetravalent uranium has a stable location in calcite (Sturchio et al. 1998). Just like Bi and Sr are related to carbonate minerals (Ionov et al.

1993; Norra et al. 2006). Also, Sr concentrated in the sediments containing aragonite (Hirst 1962) and detected in calcite (Mason 1987) and Lower Cretaceous dolomite crystals (Wogelius et al. 1992).

Factor scores association F6 (Cd–Te) elucidates 4.39% of the total variance (Tables 7 and 8) and the majority of the higher positive scores are predominantly scattered in the sediments of the Lake Nubia (Fig. 8c). The close association of both elements refers to Cd–Te solid and liquid alloys (Amzil et al. 1997) and their formation cannot be explained upon the basis of current geological knowledge because they are synthetics, most likely from anthropogenic activities in Sudan and
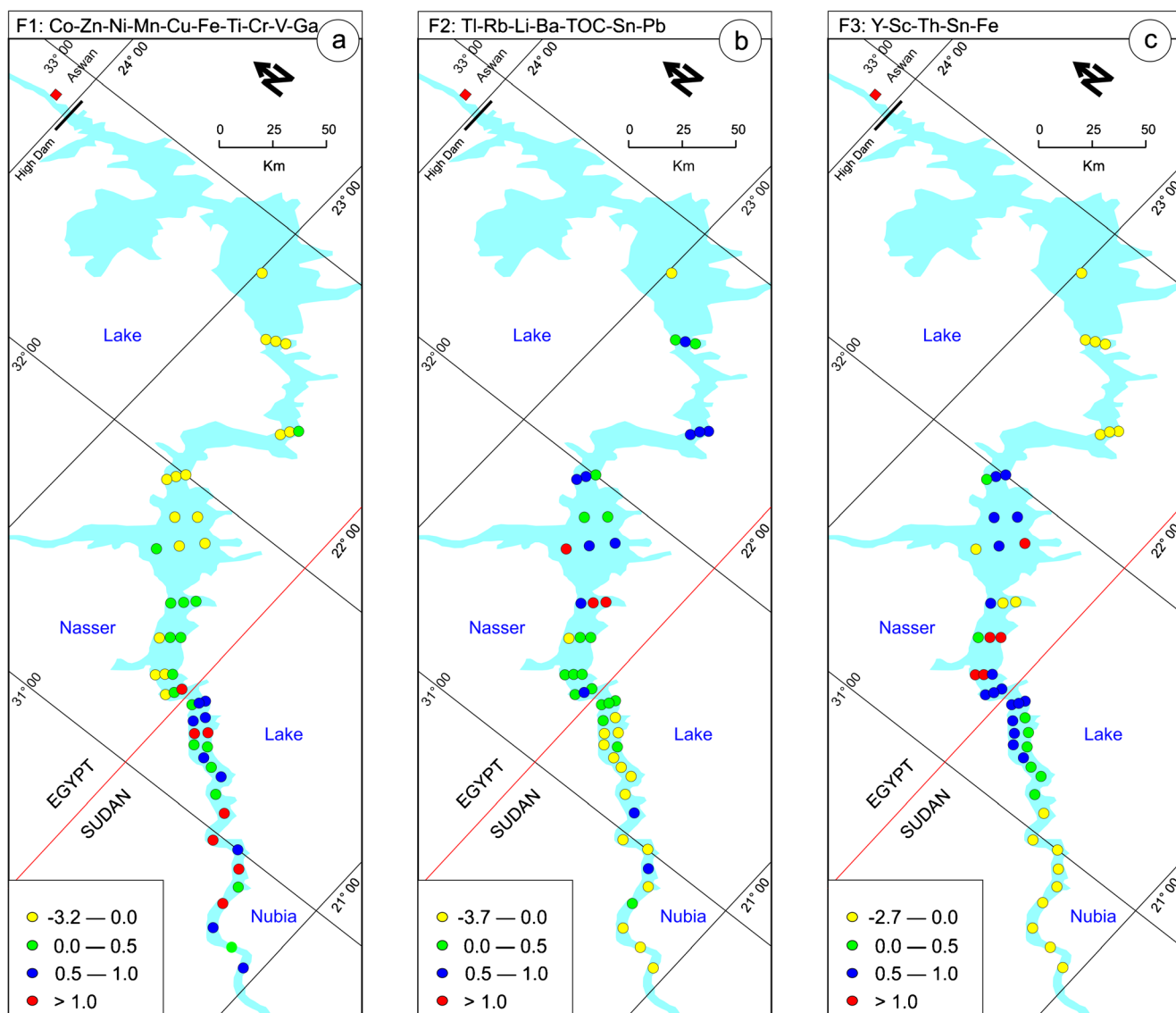
Fig. 7 Factor scores association maps (**a**–**c**) for the factors 1–3, respectively, in the bottom sediments of the High Dam Lake

the upstream Nile basin countries. These alloys can be adsorbed or trapped by clay minerals and mud fractions in the sediments (Hall et al. 1998; Reith et al. 2005) and transported northwards to few sites in the Lake Nasser.

It can be noticed that factors 2 and 5 are related to detritus carbonates and calcareous materials, despite that there is no correlation between both factors. A lack of correlation might be referred to the carbonate materials derived from different sources like Precambrian basement rocks, Tertiary limestones, Quaternary tufas, limestones, calcite, probable anthropogenic activities, and photosynthetic precipitation of $CaCO_3$. Although U and Th are distributed in both factors 3 and 5 and their concentrations exceed the average concentrations in the upper continental crust, the levels of radioactivies in the sediments and water of the whole lake are within the normal concentration ranges as mentioned by Ismail et al. (1994), Ibrahiem et al. (1995), and

Khater et al. (2005). In the scope of the findings of various statistical analyses and the spatial distributions of elements' associations, the water speed, gradient, and amount of the sediments cannot be neglected because they play more significant role in controlling the sediments geochemistry and deposition of coarse-grained fractions in the Lake Nubia and the finest in the Lake Nasser, especially in the north part.

Pollution assessment

Based on the calculation of I_{geo} values, the majority of chemical elements is clearly to be un-contaminants and characterized either by negative or low values ($I_{geo} < 1$) as shown in Table 9. Otherwise, the remaining elements, chiefly Ag, Ni, Se, and Te are generally contaminants and then the entire lake sediments can be assessed as moderate to heavily polluted
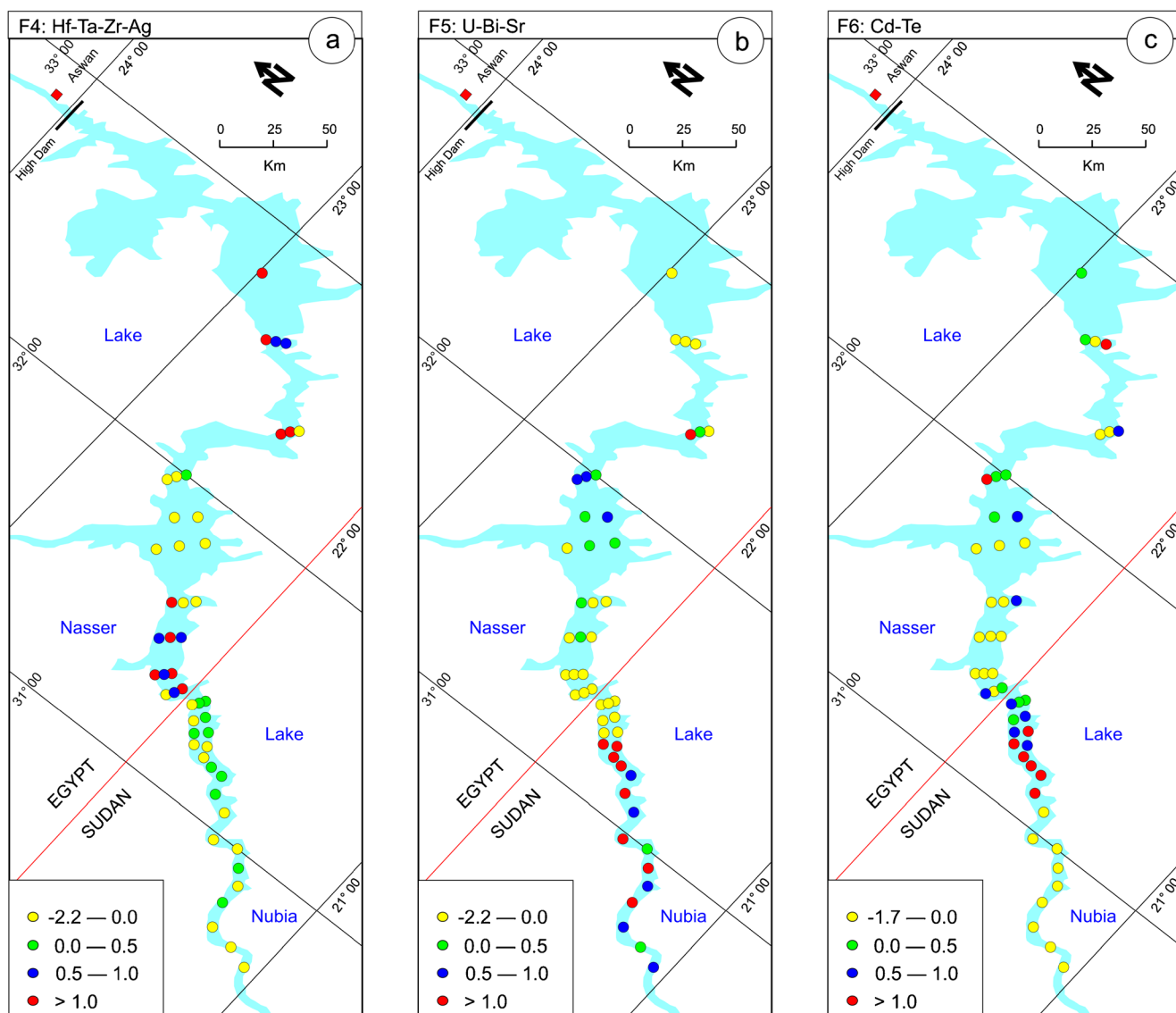
Fig. 8 Factor scores association maps (**a**–**c**) for the factors 4–6, respectively, in the bottom sediments of the High Dam Lake

with Ag and Te. It is found that the heavy pollution caused by Se was recorded in the sediments of the middle and south parts of the High Dam Lake and it enhanced, in particular, along the sediments of the north part of the lake to reach extreme pollution. Lastly, Ni yields only moderate pollution in the sediments of the Lake Nubia. According to the mean values of I_{geo}, the contaminants of interest can be arranged as follows: Se > Ag > Te > Ni.

The scale of the contamination factor and the computed results (Tables 2, 9) demonstrate that 43.3% of analyzed elements causes low contamination (CF < 1) without dangerous effect upon the sediment materials, but 56.7% of these elements enriched and turns to input various contamination levels (CF > 1) in the whole High Dam Lake sediments. Clearly, the contents of Ag, Se, and Te increased in the entire lake sediments to reach very high contamination level except Se in the middle part of the lake generate considerable

contamination. Other elements like Cd, Co, Cr, Cu, Fe, and Ga contributed moderate contamination level in the entire lake, similar to Mo and Ni in the north part; Bi, Ni, Sc, V, and Y in the middle part; and Mn, Mo, Sc, V, Y, and Zn in the south part in which Ni could reach a considerable level of contamination.

As a consequence of contamination levels, the considered contaminants reach a considerable degree of contamination in the sediments of the south and middle parts (average 58.6 and 54, respectively) and increase up to a very high degree of contamination (average 117.4) in the sediments of the north part of the lake (Table 10). For confirmation of the generated pollution and contamination, the calculated pollution load index verifies the significant pollution that caused a progressive deterioration on the entire sediments of the lake (Table 10), in spite of the surrounding area of the Lake Nasser is not recognized by the major

Table 9 Statistical results of the geoaccumulation indices and contamination factors of the analyzed elements in the High Dam Lake bottom sediments (49 samples)

Geoaccumulation indices

Element	North part					Middle part					South part				
	Minimum	Maximum	Mean	Meadian	Standard deviation	Minimum	Maximum	Mean	Meadian	Standard deviation	Minimum	Maximum	Mean	Meadian	Standard deviation
Ag	1.7	3.3	2.4	2.3	0.5	0.6	3.6	2.2	1.9	0.9	1.6	2.9	2.1	2.1	0.3
Ba	−2.8	−2.1	−2.5	−2.4	0.3	−4.2	−2.0	−2.4	−2.3	0.5	−3.5	−1.9	−2.4	−2.4	0.3
Bi	−2.9	−0.8	−2.0	−2.0	0.8	−2.1	−0.2	−0.7	−0.4	0.5	−4.7	−0.3	−1.6	−1.3	1.1
Cd	−1.3	0.7	−0.3	−0.4	0.7	−0.7	0.3	−0.4	−0.4	0.3	−1.2	−0.1	−0.4	−0.3	0.3
Co	−1.3	0.1	−0.5	−0.5	0.5	−1.3	1.2	−0.2	−0.4	0.8	0.3	1.3	0.9	0.8	0.3
Cr	−0.7	−0.2	−0.4	−0.4	0.2	−1.6	0.8	−0.2	0.2	0.5	−0.2	1.6	0.5	0.5	0.3
Cu	−0.7	0.7	0.4	0.6	0.5	−1.9	0.9	0.0	0.1	0.7	−0.3	0.9	0.4	0.5	0.3
Fe	−0.9	−0.1	−0.5	−0.5	0.3	−1.4	0.5	0.1	0.2	0.4	−0.2	0.5	0.3	0.3	0.1
Ga	−1.3	1.5	0.6	1.1	1.2	−2.2	1.8	−0.1	−0.3	1.0	−0.4	0.9	0.3	0.4	0.4
Hf	−4.2	−2.4	−3.3	−3.2	0.6	−5.8	−2.9	−3.9	−3.6	0.8	−5.3	−3.2	−4.2	−4.2	0.5
Li	−1.6	−0.9	−1.2	−1.2	0.3	−2.5	−0.4	−1.0	−1.0	0.4	−3.9	−0.9	−1.8	−1.8	0.8
Mn	−2.4	−1.0	−1.9	−1.8	0.5	−2.7	0.5	−1.0	−1.1	0.8	−0.8	0.9	0.0	0.1	0.4
Mo	−0.7	0.1	−0.3	−0.2	0.3	−3.2	−0.2	−1.8	−1.9	0.6	−3.0	4.5	−1.8	−2.0	1.5
Ni	−0.4	1.2	0.6	0.8	0.6	−1.0	1.5	0.6	1.1	0.7	0.5	1.4	1.1	1.2	0.3
Pb	−2.4	−1.0	−1.9	−1.9	0.5	−2.6	−1.2	−1.9	−2.0	0.4	−3.6	−1.4	−2.2	−2.2	0.6
Rb	−3.3	−2.3	−2.8	−2.7	0.3	−4.6	−1.7	−2.7	−2.7	0.6	−4.6	−2.1	−2.8	−2.7	0.6
Sc	−2.4	−0.7	−1.7	−1.8	0.6	−1.8	0.5	−0.3	−0.2	0.7	−1.6	0.5	−0.3	0.0	0.6
Se	4.0	6.2	5.7	5.9	0.8	0.8	5.9	3.4	3.3	1.4	3.1	4.3	3.8	3.8	0.4
Sn	−3.8	−1.9	−3.0	−2.9	0.7	−3.7	−1.4	−1.8	−1.7	0.5	−3.3	−1.5	−2.3	−2.3	0.5
Sr	−3.1	−2.3	−2.7	−2.7	0.3	−3.5	−2.8	−3.1	−3.1	0.2	−3.0	−1.9	−2.5	−2.5	0.4
Ta	−3.0	−1.1	−2.0	−2.0	0.6	−3.9	−1.6	−2.5	−2.3	0.7	−3.9	−2.0	−2.9	−2.9	0.5
Te	0.4	3.2	2.0	2.3	0.9	0.2	2.5	1.3	1.1	0.7	1.7	2.6	2.2	2.2	0.2
Th	−3.3	−1.5	−2.6	−2.6	0.6	−2.2	−0.4	−1.2	−1.1	0.4	−2.8	−1.0	−1.9	−2.0	0.4
Ti	−5.9	−2.8	−3.4	−2.9	1.1	−4.0	−1.4	−2.9	−3.1	0.6	−2.7	−0.9	−1.9	−2.0	0.4
Tl	−3.2	−2.1	−2.6	−2.7	0.4	−4.9	−1.7	−2.4	−2.2	0.7	−5.4	−1.8	−2.7	−2.5	0.9
U	−2.3	−1.0	−1.8	−1.9	0.4	−2.4	−1.1	−1.7	−1.7	0.3	−2.4	−0.6	−1.4	−1.1	0.6
V	−1.2	−0.3	−0.6	−0.6	0.3	−1.6	0.9	−0.5	−0.7	0.6	−0.3	1.7	0.6	0.5	0.5
Y	−2.0	−0.5	−1.5	−1.6	0.5	−1.5	0.3	−0.4	−0.2	0.5	−1.1	0.1	−0.4	−0.3	0.3
Zn	−1.7	−0.1	−0.8	−0.6	0.6	−2.1	−0.2	−0.9	−0.9	0.5	−0.9	0.0	−0.3	−0.3	0.2
Zr	−4.2	−3.3	−3.6	−3.5	0.3	−4.6	−2.8	−3.7	−3.7	0.6	−5.2	−2.6	−3.7	−3.7	0.6

Contamination factors

Element	North part					Middle part					South part				
	Minimum	Maximum	Mean	Meadian	Standard deviation	Minimum	Maximum	Mean	Meadian	Standard deviation	Minimum	Maximum	Mean	Meadian	Standard deviation
Ag	5.0	14.3	8.3	7.5	3.3	2.3	18.5	8.2	5.6	5.6	4.6	11.1	6.6	6.5	1.3
Ba	0.2	0.3	0.3	0.3	0.0	0.1	0.4	0.3	0.3	0.1	0.1	0.4	0.3	0.3	0.1

Table 9 (continued)

Bi	0.2	0.9	0.4	0.4	0.2	0.4	1.3	1.0	1.1	0.3	0.1	1.2	0.6	0.6	0.3
Cd	0.6	2.4	1.4	1.2	0.7	0.9	1.9	1.2	1.1	0.2	0.7	1.4	1.2	1.2	0.2
Co	0.6	1.6	1.1	1.0	0.3	0.6	3.5	1.5	1.2	0.9	1.9	3.7	2.8	2.7	0.5
Cr	1.0	1.3	1.1	1.2	0.1	0.5	2.6	1.8	1.7	0.4	1.3	4.4	2.2	2.2	0.6
Cu	0.9	2.5	2.1	2.3	0.5	0.4	2.9	1.6	1.6	0.7	1.2	2.7	2.0	2.1	0.4
Fe	0.8	1.4	1.1	1.1	0.2	0.6	2.1	1.7	1.7	0.3	1.3	2.1	1.9	1.9	0.2
Ga	0.6	4.2	2.8	3.3	1.5	0.3	5.2	1.7	1.3	1.4	1.1	2.8	1.9	2.0	0.5
Hf	0.1	0.3	0.2	0.2	0.1	0.0	0.2	0.1	0.1	0.1	0.0	0.2	0.1	0.1	0.0
Li	0.5	0.8	0.7	0.7	0.1	0.3	1.2	0.8	0.7	0.2	0.1	0.8	0.5	0.4	0.2
Mn	0.3	0.7	0.4	0.4	0.2	0.2	2.1	0.8	0.7	0.4	0.9	2.7	1.6	1.6	0.5
Mo	0.9	1.6	1.3	1.3	0.3	0.2	1.3	0.5	0.4	0.2	0.2	34.1	1.9	0.4	7.2
Ni	1.1	3.4	2.5	2.7	0.8	0.7	4.3	2.6	3.1	1.2	2.1	4.0	3.3	3.4	0.5
Pb	0.3	0.8	0.4	0.4	0.2	0.2	0.7	0.4	0.4	0.1	0.1	0.6	0.3	0.3	0.1
Rb	0.2	0.3	0.2	0.2	0.1	0.1	0.5	0.2	0.2	0.1	0.1	0.3	0.2	0.2	0.1
Sc	0.3	0.9	0.5	0.4	0.2	0.4	2.1	1.3	1.3	0.5	0.5	2.1	1.3	1.5	0.5
Se	24.1	112.8	86.4	87.6	30.2	2.7	90.0	24.7	15.1	26.0	12.6	30.2	21.4	20.3	5.3
Sn	0.1	0.4	0.2	0.2	0.1	0.1	0.6	0.4	0.4	0.1	0.2	0.5	0.3	0.3	0.1
Sr	0.2	0.3	0.2	0.2	0.1	0.1	0.2	0.2	0.2	0.0	0.2	0.4	0.3	0.3	0.1
Ta	0.2	0.7	0.4	0.4	0.2	0.1	0.5	0.3	0.3	0.1	0.1	0.4	0.2	0.2	0.1
Te	2.0	13.8	7.0	7.2	4.0	1.8	8.5	4.0	3.2	2.0	4.7	9.0	6.9	6.9	1.1
Th	0.2	0.5	0.3	0.2	0.1	0.3	1.1	0.7	0.7	0.2	0.2	0.7	0.4	0.4	0.1
Ti	0.0	0.2	0.2	0.2	0.1	0.1	0.6	0.2	0.2	0.1	0.2	0.8	0.4	0.4	0.1
Tl	0.2	0.3	0.2	0.2	0.1	0.0	0.5	0.3	0.3	0.1	0.0	0.4	0.3	0.3	0.1
U	0.3	0.8	0.5	0.4	0.2	0.3	0.7	0.5	0.5	0.1	0.3	1.0	0.6	0.7	0.2
V	0.7	1.2	1.0	1.0	0.2	0.5	2.9	1.2	1.0	0.6	1.2	4.8	2.4	2.2	0.8
Y	0.4	1.0	0.6	0.5	0.2	0.5	1.8	1.2	1.3	0.3	0.7	1.6	1.2	1.3	0.2
Zn	0.5	1.4	0.9	1.0	0.3	0.3	1.3	0.8	0.8	0.3	0.8	1.5	1.2	1.2	0.2
Zr	0.1	0.2	0.1	0.1	0.0	0.1	0.2	0.1	0.1	0.1	0.0	0.2	0.1	0.1	0.1

Table 10 Statistical results of the contamination degrees and pollution load indices of the heavy elements in the High Dam Lake bottom sediments (49 samples)

	Contamination degrees						Pollution load indices					
	Minimum	Maximum	Mean	Median	Standard deviation	Contamination degree	Minimum	Maximum	Mean	Median	Standard deviation	Pollution level
North part	53.3	148.6	117.4	117.7	31.4	Very high	1.4	2.2	1.8	1.8	0.3	Polluted
Middle part	30.2	126.1	54.0	46.5	25.9	Considerable	0.8	2.5	1.8	1.8	0.4	Polluted
South part	45.4	90.1	58.6	58.0	9.8	Considerable	1.8	3.2	2.3	2.3	0.3	Polluted

pollution sources (e.g., rural or urban communities, highways, agricultural and industrial activities). Undoubtedly, the produced pollution has come from south Egypt, Sudan, and the upper Nile basin countries as a result of natural enrichment of geogenic processes including weathering of various rock units, soil erosion, and an atmospheric deposition of aerosols containing metals. Also, it has come from anthropogenic activities represented by emissions, liquid and solid waste materials of industries, mining activities, vehicles, locomotives, power stations, ships and fishing boats, cultivations, and domestic sewage systems of urbanization and unplanned rural activities in the Sudan and the upper Nile basin countries (George and Elmoghraby 1978; El Zorgani et al. 1979; Abdel Magid et al. 1984; Ali 1999; Saeed 2004; Bastawy 2007; Ministry of Environment and Physical Development 2007).

Overall, the investigated bottom lake sediments are low-quality and not free of potential environmental hazards, and may create a potential risk to the ecosystem and can not be accepted as safe materials. Thus, the present evaluation is not in agreement with suggestion of Goher et al. (2014) who revealed that the Egyptian Lake Nasser sediments may be represented as a reference to a pre-industrial background of the River Nile sediments. It is most important to conclude that the remarkable geochemical record and distribution of sediments, and behavior, levels, and dispersion patterns of the analyzed elements in the intact High Dam Lake were influenced by the geology, weathering processes, amount and composition of the sediments, sorting during transportation and deposition processes, volume and velocity of water, organic carbon, pH, windblown sand, anthropogenic inputs, and geographic factors. In addition, other important factors can not be ignored like focusing processes during transportation, sedimentation, and post-depositional reactions (Jin et al. 2006), fluvial sedimentation-controlling trace elements distribution in the sediments (Zaghloul et al. 1987), Eh of water influencing trace elements deposition (El Dardir et al. 1988), environmental parameters (temperature, salinity, hardness, dissolved oxygen, etc.) affecting on their accumulation (Elewa et al. 1990), and the flood and drought periods.

In the scope of the global price of the valuable elements and modern technology for exploitation and extraction operations, the prolific huge amounts of the investigated sediments are fruitful and can be used as natural fertilizers with/without remediation for improvement of quality of desert soils around the High Dam Lake, raw materials for building materials, bricks, ceramic and refractory industries, and a source the valuable elements and minerals. The follow-up works using core sampling techniques are recommended in order to perform further evaluation of these sediments in the future. Also, the created new Nile delta between north Sudan and south Egypt should be subjected to further investigation.

Conclusion

The prolific enormous amounts of the sediments in the whole High Dam Lake act as good accumulators for trace elements derived from natural origin and anthropogenic activities. The geochemical evaluation of analyzed variables in these sediments gives a clear image and comprehensive understanding of the geochemical record and spatial distribution of sediments, behavior, baseline levels, and dispersion patterns of the considered elements and related contribution sources, and their mechanism of concentrations, deposition, and association in the whole High Dam Lake. Generally, the statistical techniques could successfully discriminate the elements causing enrichments, and element association, distinguished the sediments of the lake parts, exhibited correlation of sediments geochemistry with their composition in accordance with geology of the study area, geogenic processes, environmental parameters, anthropogenic activities, and geographic positions of the Nile basin countries. In brief, the present study carries positive signatures and promises for economic significance and environmental assessment. Since, it encourages the private and governmental companies to extract valuable elements/minerals and use these sediments in various industries and a new land reclamation. Environmentally, the mentioned sediments can not be accepted as a reference to a pre-industrial background of the River Nile sediments because they are actually polluted.

References

Abdel Magid HM, Ibrahim IS, Dirar HA (1984) Chemical and microbiological examination of well and Nile water. Environ Int 10(3):259–263

Abou El Ella SM, El Samman TA (2010) Ecosystem status of the north part of Lake Nubia. Sudan African J Biol Sci 6(2):7–21

Ahmed EA, El-Dardir M, Gindy NN (1993) Sedimentological, mineralogical and geochemical studies on some recent Khors sediments, Lake Nasser, Egypt. J Afr Earth Sci 17(3):383–397

Ali S (1999) Greater Khartoum: the horizontal expansion and its impact on the development of settlement. MA Thesis, Khartoum University, Sudan (in Arabic)

Amzil A, Mathieu JC, Castanet R (1997) Calorimetric investigation on the Cd -Te binary alloys. J Alloys Comp 258:192–195

Asami M, Suzuki K, Grew ES (2002) Chemical Th–U–total Pb dating by electron microprobe analysis of monazite, xenotime and zircon from the Archean Napier complex, East Antarctica: evidence for ultra-high-temperature metamorphism at 2400 Ma. Precambrian Res 114(3–4):249–275

Ávila PF, Oliveira JMS, Ferreira da Silva E, Fonseca EC (2005) Geochemical signatures and mechanisms of trace elements dispersion in the area of the Vale das Gatas mine (northern Portugal). J Geochem Explor 85:17–29

Awadallah RM, Ismail SS, Arifien E, Moalla SM, Grass F (1994) Distribution of trace elements in mud sediments of Aswan high dam Lake. Chem Erde 54:67–82

Bastawy O (2007) Effect of Khartoum City for water quality of the River Nile. M.Sc. Thesis, Linköpings Universitet, Sweden

Bhuiyan MAH, Parvez L, Islam MA, Dampare SB, Suzuki S (2010) Heavy metal pollution of coal mineaffected agricultural soils in the northern part of Bangladesh. J Hazard Mater 173:384–392

Bianchi TS, Mitra S, McKee BA (2002) Sources of terrestrially-derived organic carbon in lower Mississippi River sediments: implications for differential sedimentation and transport at the coastal margin. Mar Chem 77:211–223

Boshnaq MH (2012) Sedimentary accretion of windblown sand along wesern bank of Lake Nasser. M.Sc. Thesis, South Valley University, Qena, Egypt

Cabrera F, Clemente L, Barrientos DE et al (1999) Heavy metal pollution of soils affected by the guadiamar toxic flood. Sci Total Environ 242(1—3):117–129

Caeiro S, Costa MH, Ramos TB (2005) Assessing heavy metal contamination in Sado estuary sediment: an index analysis approach. Ecol Indic 5:151–169

Chakravarty M, Patgiri AD (2009) Metal pollution assessment in sediments of the Dikrong River, N.E. India. J Hum Ecol 27(1):63–67

Conoco (1987) Geologic Map of Egypt. Egyptian General Authority for Petroleum (UNESCO joint map project) 20 sheets scale 1:500 000 Cairo Egypt

Darwish MAG (2013) Geochemistry of the high dam Lake sediments, South Egypt: implications for environmental significance. Int J Sed Res 28:544–559

Davis JA, Leckie JO (1978) Surface ionization and complexation at the oxide/water interface II. Surface properties of amorphous iron oxyhydroxide and adsorption of metal ions. J Colloid Interface Sci 67(1):90–107

de Barros CE, Nardi LVS, Dillenburg SR, Ayup R, Jarvis K, Baitelli R (2010) Detrital minerals of modern beach sediments in southern Brazil: a provenance study based on the chemistry of zircon. J Coast Res 26(1):80–93

Eisler R (1996) Silver hazards to fish, wildlife, and invertebrates: a synoptic review. Biological Report 32 Laurel USA: US National Biological Service Patuxent Wildlife Research Center

El Dardir M (1984) Geochemical and sedimentological studies on the sediments of Aswan high Dam Reservoir. Ph. D. Thesis, Al Azhar University, Cairo, Egypt

El Dardir M (1987) Sedimentation processes in Lake Nubia. Bull Inst Oceanogr & Fish ARE 13(2):53–64

El Dardir M (1994) Sedimentation in Nile high dam reservoir, 1987-1992, and sedimentary futurologic aspects. Sedimentol Egypt 2:23–39

El Dardir M, Hathout MH, Hassan MM (1988) Distribution of the chemical components in the sediments of the Khors of the Aswan high dam reservoir, Egypt. Bull Fac Sci Zagazig Univ 10:133–150

Elewa AA, Sayyah SM, Fouda A (1990) Distribution of some pollutants in Lake Nasser and River Nile at Aswan (ed. El- Raey M), Regioonal Symp. Environ. Stud. (UNARL), Alexandria

El Gaby S (1985) On the relation between tectonics and ore mineral occurrences in the basement complex of the Eastern Desert of Egypt. Proc. 6th Int. Conf. Basement Tectonics, Santa Fe, pp 652–671

El Gaby S, List F, Tehrani R (1990) The basement complex of the Eastern Desert and Sinai. In: Said R (ed) The geology of Egypt. Balkema, Rotterdam, p 175

El Ramly M, Hussein A (1985) The ring complexes of the Eastern Desert of Egypt. J Afr Earth Sci 3:77–82

Elsawwaf M, Feyen J, Batelaan O, Bakr M (2012) Groundwater–surface water interaction in Lake Nasser, southern Egypt. Hydrol Process https://doi.org/10.1002/hyp.9563

El-Shabrawy GM (2009) Lake Nasser–Nubia. In: Dumont HJ (ed.) The Nile: origin, environments, limnology and human use, Springer Science + Business Media B.V., pp 125–155

El Zorgani GA, Abulla AM, Ali MET (1979) Residues of organochlorine insecticides in fishes in Lake Nubia. Bull Environ Contam Toxicol 22:44–48

Entz BAG (1974) Report on the lomnological conditions of Lake Nasser. In the report to Lake Nasser and Lake Nubia. Working Paper No. 6 (LNDCRPA) Aswan, Egypt

Entz BAG (1980) Sedimentation processes in the reservoir Lake Nasser-Nubia during 1965-1974 and future aspects. Water supply and management. Pergamon Press Ltd, Oxford 4: 67–72

Gaebler H (1997) Mobility of heavy metals as a function of pH of samples from an overbank sediment profile contaminated by mining activities. J Geochem Explor 58:185–194

Garzanti E, Andò S, Padoan M, Vezzoli G, El Kammar A (2015) The modern Nile sediment system: processes and products. Quat Sci Rev 130:9–56

Garzanti E, Andò S, Vezzoli G, Abdel Megid AA, El Kammar A (2006) Petrology of Nile River sands (Ethiopia and Sudan): sediment budgets and erosion patterns. Earth Planet Sci Lett 252:327–341

Gaspar JC, Wyllie PJ (1984) The alleged kimberlite-carbonatite relationship: evidence from ilmenite and spinel from premier and Wesselton mines and the Benfontein sill, South Africa. Contrib Mineral Petrol 85:133–140

George TT, Elmoghraby AI (1978) Status of aquatic pollution in the Sudan, its control and protection of the living resources. Sixth FAO/SIDA Workshop on aquatic pollution in relation to protection of living resources FIR:TPLR/78/Inf.20

Gindy NN (1991) Mineralogical, geochemical and sedimentlogical studies on some Khors sediments of Lake Nasser, M.Sc. Thesis, Assiut University, Egypt

Gindy NN (2001) Mineralogical, geochemical and sedimentlogical characteristics of Lake Nasser sediments, Egypt. Ph.D. Thesis, Assiut University, Egypt

Gindy NN (2015) Environmental implications of electron microscope study of quartz grains' surface textures on khors sediments, Lake Nasser, Egypt. Egypt J Aquat Res 41:41–47

Goher ME, Farhat HI, Abdo MH, Salem SG (2014) Metal pollution assessment in the surface sediment of Lake Nasser, Egypt. Egypt J Aquat Res 40:213–224

Gramacciol CM, Segalstad TV (1978) A uranium-and thorium-rich monazite from a south-alpine pegmatite at Piona. Italy Am Mineral 63: 757–761

Grassian VH (2001) Heterogeneous uptake and reaction of nitrogen oxides and volatile organic compounds on the surface of atmospheric particles including oxides, carbonates, soot and mineral dust: implications for the chemical balance of the troposphere. Int Rev Phys Chem 20(3):467–548

Hakanson L (1980) An ecological risk index for aquatic pollution control. A sedimentological approach. Water Res 14:975–1001

Hall GEM, MacLaurin AI, Garrett RG (1998) Assessment of the 1 M NH_4NO_3 extraction protocol to identify mobile forms of Cd in soils. J Geochem Explor 64 (1–3): 153–159

Harman HH (1970) Modern factor analysis. In: University of Chicago Press. Chicago, USA

Hassan F, Abu Zeid M, Hafez K (1977) Mineralogical composition of the clay fraction of the High dam Lake sediments. Lake Naser and River Nile Project, prepared for Acad of Sci Res and Tech Egypt

Hedges JI, Keil RG (1995) Sedimentary organic matter preservation: an assessment and speculative synthesis. Mar Chem 49:81–115

Hirst DM (1962) The geochemistry of modern sediments from the Gulf of Paria—II the location and distribution of trace elements. Geochim Cosmochim Acta 26(11):1147–1187

Holmström H, Öhlander B (2001) Layers rich in Fe- and Mn-oxyhydroxides formed at the tailings-pond water interface, a possible trap for trace metals in flooded mine tailings. J Geochem Explor 74(1/3):189–203

Hu Z, Gao S (2008) Upper crustal abundances of trace elements: a revision and update. Chem Geol 253(3):205–221

Ionov DA, Dupuy C, O'Reilly SY, Kopylova MG, Genshaft YS (1993) Carbonated peridotite xenoliths from Spitsbergen: implications for trace element signature of mantle carbonate metasomatism. Earth Planet Sci Lett 119(3):283–297

Ibrahiem MN, Shawky S, Amer HA (1995) Radioactivity levels in Lake Nasser sediments. Appl Radiat Isot 46(5):297–299

Ismail SS, Unfried E, Grass F (1994) Distribution of 137 Cs and 228 Ra in the sediments of Aswan high dam lake. J Radioanal Nucl Chem 186(2):143–155

Issawi B (1982) Geology of the southwestern desert of Egypt. Ann Geol Surv Egypt 11:57–66

Jiang SY, Yu JM, Lu JJ (2004) Trace and rare-earth element geochemistry in tourmaline and cassiterite from the Yunlong tin deposit, Yunnan, China: implication for migmatitic–hydrothermal fluid evolution and ore genesis. Chem Geol 209(3–4):193–213

Jin Z, Li F, Cao J, Wang S, Yu J (2006) Geochemistry of Daihai Lake sediments, Inner Mongolia, North China: implications for provenance, sedimentary sorting, and catchment weathering. Geomorphology 80:147–163

Kaiser K, Zech W (2000) Dissolved organic matter sorption by mineral constituents of subsoil clay fractions. J Plant Nutr Soil Sci 163(5): 531–535

Khalifa EM, Soliman MA, Asdek HS (1994) Mineralogical characteristics of the high dam Lake sediments. Bull Fac Sci Assiut Univ 23(2-F):251–284

Khater AE, Ebaid YY, El-Mongy SA (2005) Distribution pattern of natural radionuclides in Lake Nasser bottom sediments. Int Congr Ser 1276:405–406

Khudeir A (1983) Geology of the ophiolite suite of El Rubshi area, Eastern Desert, Egypt. Ph D thesis, Assiut University, Egypt

Klitzsch E, List FK, Poehlmann G (1987) Geological map of Egypt. 20, Sheets, scale 1: 500.000. The Egyptian General Petroleum Corporation (EGPC) and CONOCO

Land M, Thunberg J, Öhlander B (2002) Trace metal occurrence in a mineralised and a non-mineralised spodosol in northern Sweden. J Geochem Explor 75(1–3):71–91

Liu WH, Zhao JZ, Ouyang ZY, Soderlund L, Liu GH (2005) Impacts of sewage irrigation on heavy metal distribution and contamination in Beijing, China. Environ Int 31:805–812

Makary AZ, El-Moattassem M, Fahmy A (2004) Evaluation of Lake Nasser environmental sedimentation (1964-2000). In: Hu C, Tan Y, Zhou Z, Shao X, Liu C (eds) Proceedings of the ninth international symposium on river sedimentation 1–4: 917–923

Mancy KH, Hafez M (1983) Water quality and ecosystem considerations in integrated Nile resources management. In: Elassiouti IM, Marks DH (eds) Water resources planning in Egypt. Ministry Irrigation, Cairo, pp 469–485

Martin TD, Creed JT, Brockhoof CA (1994) Method 200.2 (revision 2.8): sample preparation procedure for spectrochemical determination of total recoverable elements. In: Methods for the determination of metals in environmental samples, USEPA, Cincinnati, Ohio 45268

Masau M, Černý P, Chapman R (2000) Exsolution of zirconian-hafnian wodginite from manganoan-tantalian cassiterite, annie claim #3 granitic pegmatite, southeastern Manitoba, Canada. Can Mineral 38(3): 685–694

Mason RA (1987) Ion microprobe analysis of trace elements in calcite with an application to the cathodoluminescence zonation of limestone cements from the lower carboniferous of South Wales, U.K. Chem Geol 64(3–4):209–224

McKnight TL, Hess D (2000) "Climate zones and types". Physical geography: a landscape appreciation. Upper Saddle River: Prentice Hall. ISBN 0-13-020263-0

Ministry of Environment and Physical Development (2007) Higher council for environment and natural resources National implementation plan for the Stockholm convention on POPs, Sudan. p. 190

Moalla SMN, Awadallah RM, Rashed MN, Soltan ME (1997) Distribution and chemical fractionation of some heavy metals in bottom sediments of Lake Nasser. Hydrobiologia 364(1):31–40

Moussa AMA (2013) Predicting the deposition in the Aswan high dam reservoir using a 2-D model. Ain Shams Eng J 4:143–153

Mücke A, Bhadra Chaudhuri JN (1991) The continuous alteration of ilmenite through pseudorutile to leucoxene. Ore Geol Rev 6(1):25–44

Müller G (1979) Schwermetalle in den Sedimenten des Rheines-Veränderungen seit 1971. Umschau 79:778–785

Müller G (1981) Die Schwermetallbelstung der sedimente des Neckars und seiner Nebenflusse: eine Bestandsaufnahme. Chemiker-Zeitung 105:157–164

Ng SL, King RH (2004) Geochemistry of Lake sediments as a record of environmental change in a high arctic watershed. Chem Erde 64: 257–275

Nile Basin Initiative Transboundary Environmental Action Project (2005). National Nile basin water quality monitoring baseline report for Sudan, March 2005, p 39

Norra S, Lanka-Panditha M, Kramar U, Stüben D (2006) Mineralogical and geochemical patterns of urban surface soils, the example of Pforzheim, Germany. Appl Geochem 21:2064–2081

Norusis MJ (1988) SPSS introductory statistics guide. In: SPSS incorporation. Chicago, USA

Padoan M, Garzanti E, Harlavan Y, Villa IM (2011) Tracing Nile sediment sources by Sr and Nd isotope signatures (Uganda, Ethiopia, Sudan). Geochim Cosmochim Acta 75:3627–3644

Park CI, Cha KW (1999) Spectrophotometric determination of scandium (III) in monazite after separation using amberlite IRC 718 chelating resin. Bull Kor Chem Soc 20(12):1409

Pekey H, Karakaş D, Ayberk S, Tolun L, Bakoğlu M (2004) Ecological risk assessment using trace elements from surface sediments of Izmit Bay (northeastern Marmara Sea) Turkey. Mar Pollut Bull 48:946–953

Philip G, Hassan F, Khalil J (1977) Mechanical analysis and mineral composition of Lake Nasser. Lake Nasser and River Nile project, Report prepared for the Acad of Sci Res and Tech, Egypt

Pokrovsky OS, Schott J (2002) Iron colloids/organic matter associated transport of major and trace elements in small boreal rivers and their estuaries (NW Russia). Chem Geol 190(1–4):141–179

Prost R, Koutit T, Benchara A, Huard E (1998) State and location of water adsorbed on clay minerals: consequences of the hydration and swelling-shrinkage phenomena. Clay Clay Miner 46(2):117–131

Ranasinghe PN, Fernando GWAR, Dissanayake CB, Rupasinghe MS, Witter DL (2009) Statistical evaluation of stream sediment geochemistry in interpreting the river catchment of high-grade metamorphic terrains. J Geochem Explor 103:97–114

Rantitsch G (2004) Geochemical exploration in a mountainous area by statistical modeling of polypopulational data distributions. J Geochem Explor 82:79–95

Rao MM (1963) Discriminant analysis. Ann Inst Stat Math 15(1):11–24

Rath P, Panda UC, Bhatta D, Sahu KC (2009) Use of sequential leaching, mineralogy, morphology and multivariate statistical technique for quantifying metal pollution in highly polluted aquatic sediments—a case study: Brahmani and Nandira Rivers, India. J Hazard Mater 163:632–644

Reedman JH (1979) Techniques in mineral exploration. Applied Science Publishers, London

Reimann C, Filzmoser P, Garrett PG (2002) Factor analysis applied to regional geochemical data: problems and possibilities. Appl Geochem 17:185–206

Reith F, Mc Phail DC, Christy AG (2005) Christy Bacillus cereus, gold and associated elements in soil and other regolith samples from Tomakin Park gold mine in southeastern New South Wales. Austr J Geochem Explor 85:81–98

Rovira M, Giménez J, Martínez M, Martínez-Lladó X, de Pablo J, Martí V, Duro L (2008) Sorption of selenium (IV) and selenium (VI) onto natural iron oxides: goethite and hematite. J Hazard Mater 150(2): 279–284

Rožić M, Cerjan-Stefanović Š, Kurajica S, Vančina V, Hodžić E (2000) Ammoniacal nitrogen removal from water by treatment with clays and zeolites. Water Res 34(14,1):3675–3681

Sadiek HS (1987) Granulometry and mineralogy of the nile sediment in the High Dam Lake with special reference to Lake Nubia. M. Sc. Thesis, Assiut University, Egypt

Saeed ZO (2004) The effects of the water quality on freshwater fauna and flora around Khartoum. Ph.D. thesis, University of Khartoum, Sudan

Sahu KC, Mukherjii PK (1983) Monitoring of water and sediments of Ulhas river. Northeast Mumbai Mahasagar 16:135–142

Said R (1990) Geomorphology. In: Said R (ed) The geology of Egypt. Balkema, Rotterdam, pp 9–25

Schroeder PA, Le Golvan JJ, Roden MF (2002) Weathering of ilmenite from granite and chlorite schist in the Georgia Piedmont. Am Mineral 87(11–12):1616–1625

Sefelnasr A M (2007) Development of groundwater flow model for water resources management in the developement areas of the Western Desert, Egypt. Ph.D. thesis, Martin Luther University, Halle-Wittenberg, Germany

Shaltout MAM (1998) Solar hydrogen from Lake Nasser for 21st century in Egypt. Int J Hydrog Energy 23(4):233–238

Sherief MK, Awadallah RM, Grass F (1978) Trace elements in sediment samples in Lake Nasser–Lake Nubia. Bull Fac Sci Assiut Univ 7: 363–378

Strzepek KM, Yohe GW, Tol RSJ, Rosegrant MW (2008) The value of the high Aswan dam to the Egyptian economy. Ecol Econ 66:117–126

Sturchio NC, Antonio MR, Soderholm L, Sutton SR, Brannon JC (1998) Tetravalent Uranium in Calcite. Science 281(5379):971–973

Suresh Babu DS, Thomas KA, Mohan Das PN, Damodaran AD (1994) Alteration of ilmenite in the Manavalakurichi deposit. India Clays and Clay Miner 42(5):567–571

Suresh G, Ramasamy V, Meenakshisundaram V, Venkatachalapathy R, Ponnusamy V (2011) Influence of mineralogical and heavy metal composition on natural radionuclide contents in the river sediments. Appl Radiat Isot 69:1466–1474

Taylor SR, McLennan SM (1985) The Continental Crust: Its Composition and Evolution. Blackwell Scientific Boston Mass

Taylor SR, McLennan SM (1995) The geochemical evolution of the continental crust. Rev Geophys 33(2):241–265

Thomas MM, Clouse JA, Longo JM (1993) Adsorption of organic compounds on carbonate minerals: 1. Model compounds and their influence on mineral wettability. Chem Geol 109(1–4):201–213

USGS (2004) SRTM data, USGS Seamless Data Distribution System-Enhanced. United States Geological Survey, http://srtm.usgs.gov. Last accessed: March 2007

Wogelius RA, Fraser DG, Feltham DJ, Whiteman MI (1992) Trace element zoning in dolomite: proton microprobe data and thermodynamic constraints on fluid compositions. Geochim Cosmochim Acta 56(1):319–334

Xiangping L, Fei Z, Jianying Q, Yongheng C (2012) Effects of organic matter on thallium adsorption-desorption in soils. Chin J Environ Eng 6(11):4245–4250

Yilmaz H (2003) Geochemical exploration for gold in western Turkey: success and failure. J Geochem Explor 80:117–135

Zaghloul Z.M, El-Reedy E, Dardir M, El-Massry A, Hassan MM (1987) Distribution of the heavey metal in the bottom sediment of Aswan high dam reservoir (abstract), fifth annual meeting of the Geol Soc of Egypt, Cairo

Zaki SR (2009) Geoenvironmental impact of the Aswan High Dam and reclamation project on the groundwater condition in the area to the west of the High Dam Lake, Egypt. Ph.D. Thesis, Sohag University, Egypt